Ruptures sismiques en supershear:
du terrain au laboratoire

Alexandre SCHUBNEL

Laboratoire de Géologie, CNRS - Ecole Normale Supérieure, Paris France

ACKNOWLEDGEMENTS

@ ENS: François Passelègue, Raul Madariaga

@ IPGP: Harsha Bhat

@ INGV Roma: Stefan Nielsen

MOTIVATION

A schematic view of earthquake nucleation and propagation

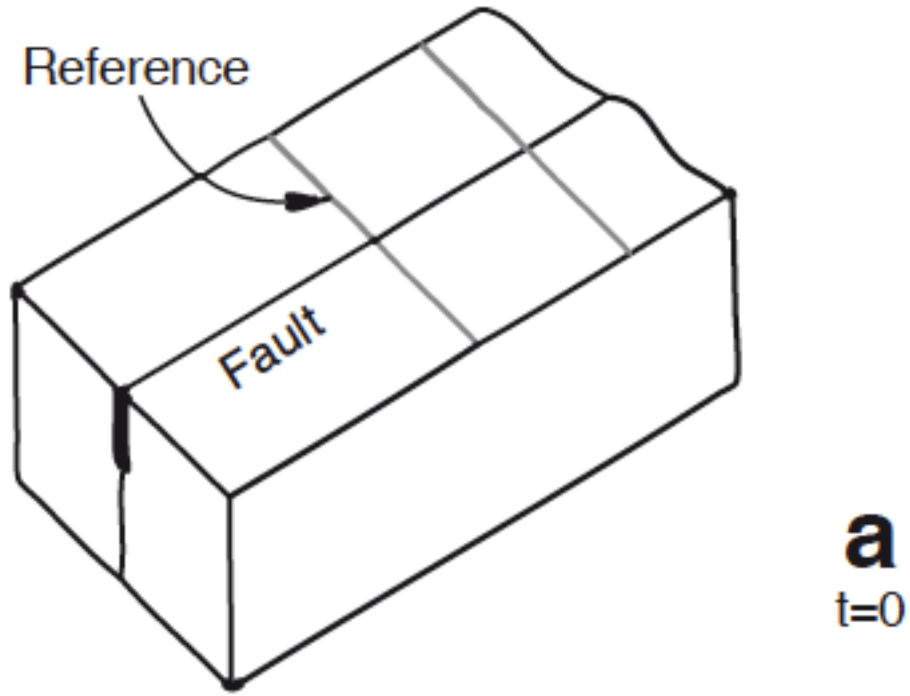

MOTIVATION

A schematic view of earthquake nucleation and propagation

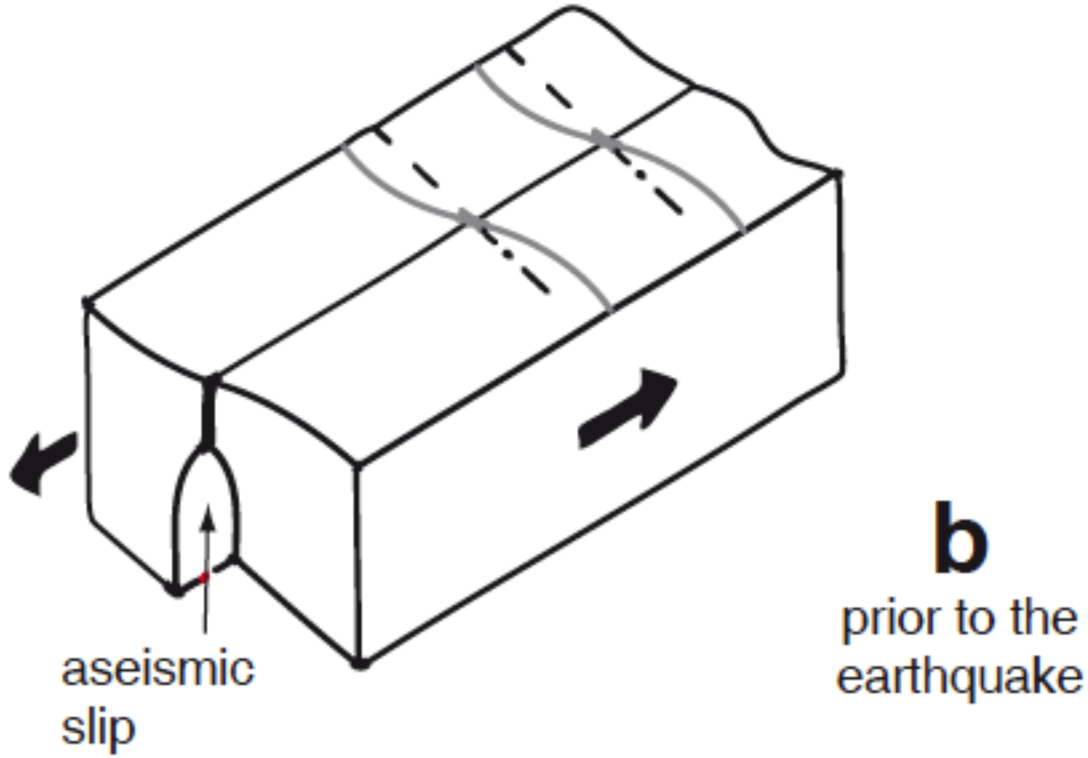

MOTIVATION

A schematic view of earthquake nucleation and propagation

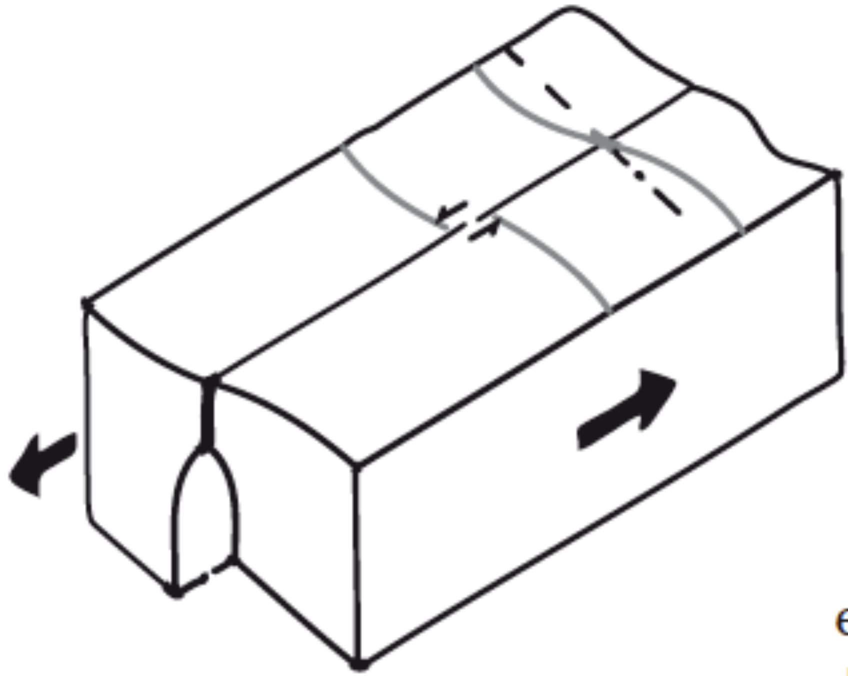

c
earthquake
nucleation

MOTIVATION

A schematic view of earthquake nucleation and propagation

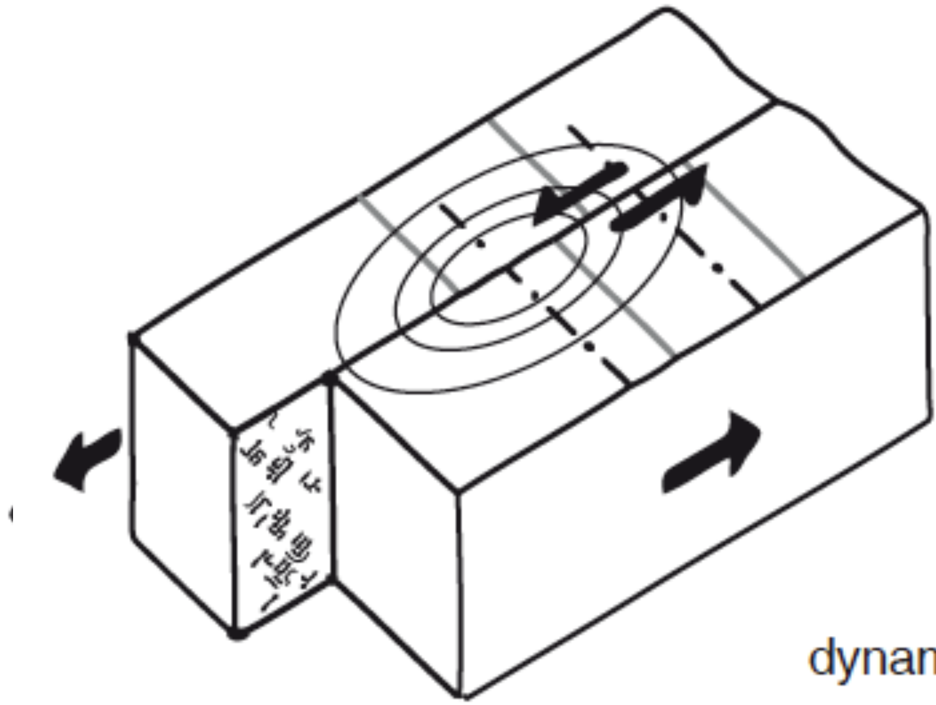

d
dynamic rupture
and slip

MOTIVATION

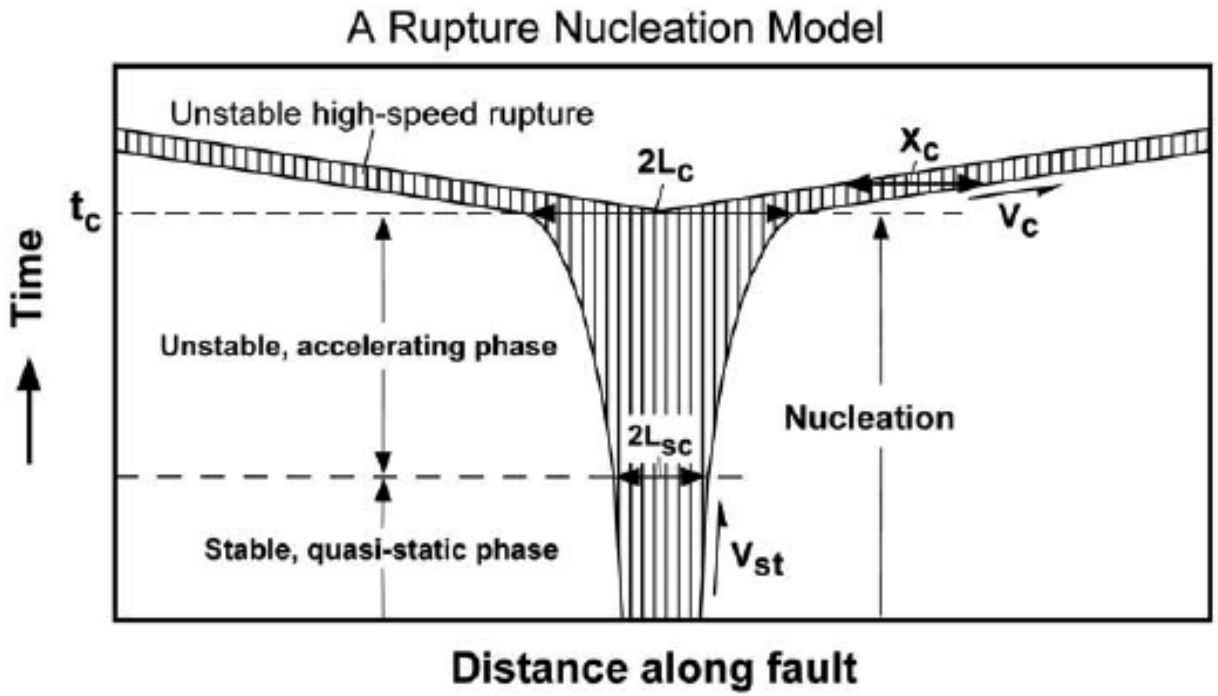

Figure 15. A physical model of rupture nucleation. Hatched portion indicates the zone in which the breakdown (or slip-weakening) proceeds with time.

Ohnaka 2003

MOTIVATION

EQ “damage” (strong ground motion + radiated waves) depends directly on the rupture velocity

Radiation efficiency vs. Rupture speed

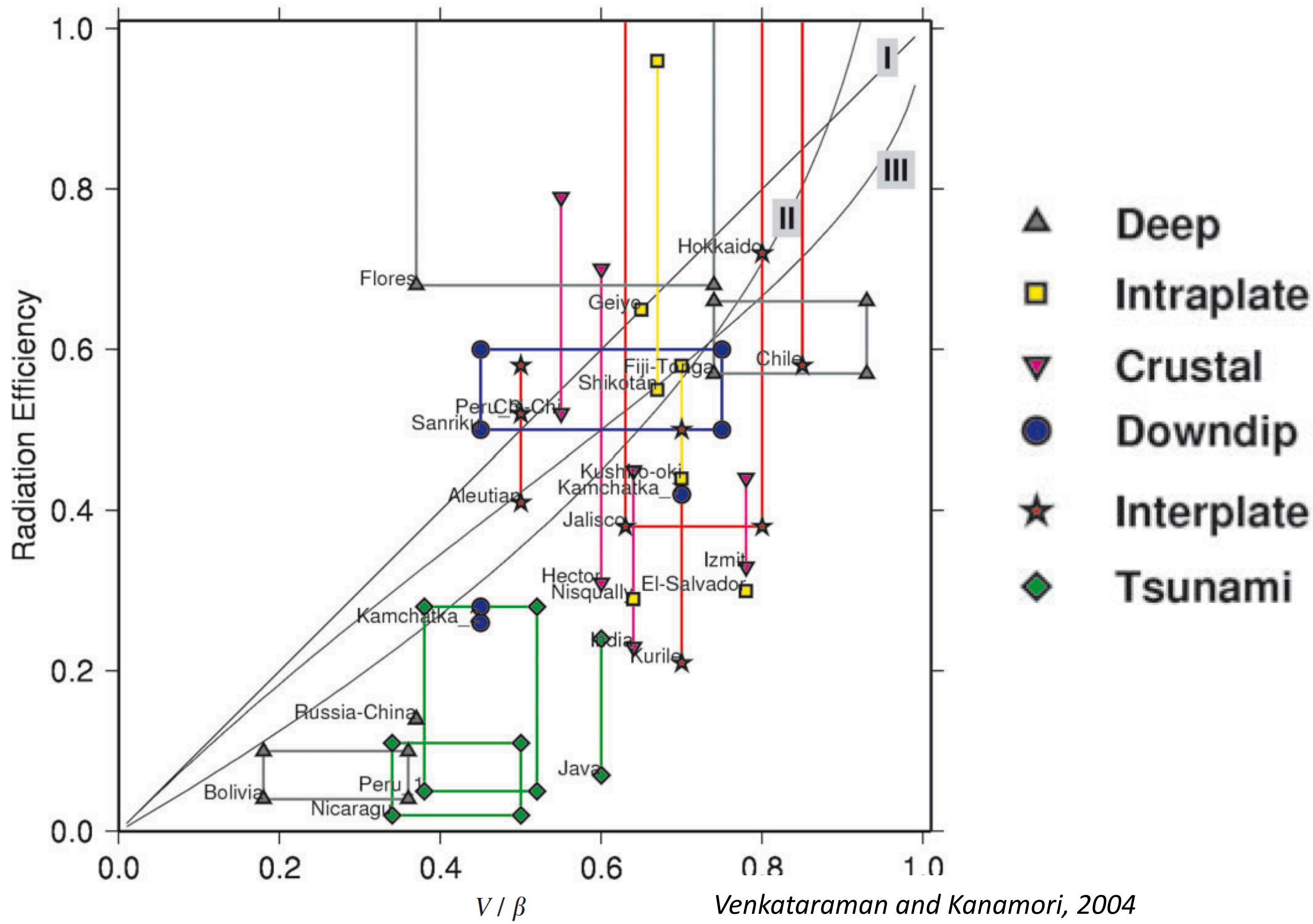

Venkataraman and Kanamori, 2004

MOTIVATION

Six **strike-slip** earthquakes have been documented up to now:
Imperial valley *(Mw=6.5 Ca. USA, 1979)*, Izmit *(Mw=7.6, Turkey 1999)*, Duzce *(Mw=7.2 Turkey, 2000)*, Kulunshan *(Mw=8.1, China, 2001)*, Denali *(Mw= 7.9, Alaska, USA,2002)*, Indian Ocean *(Mw=8.6, 2012)*

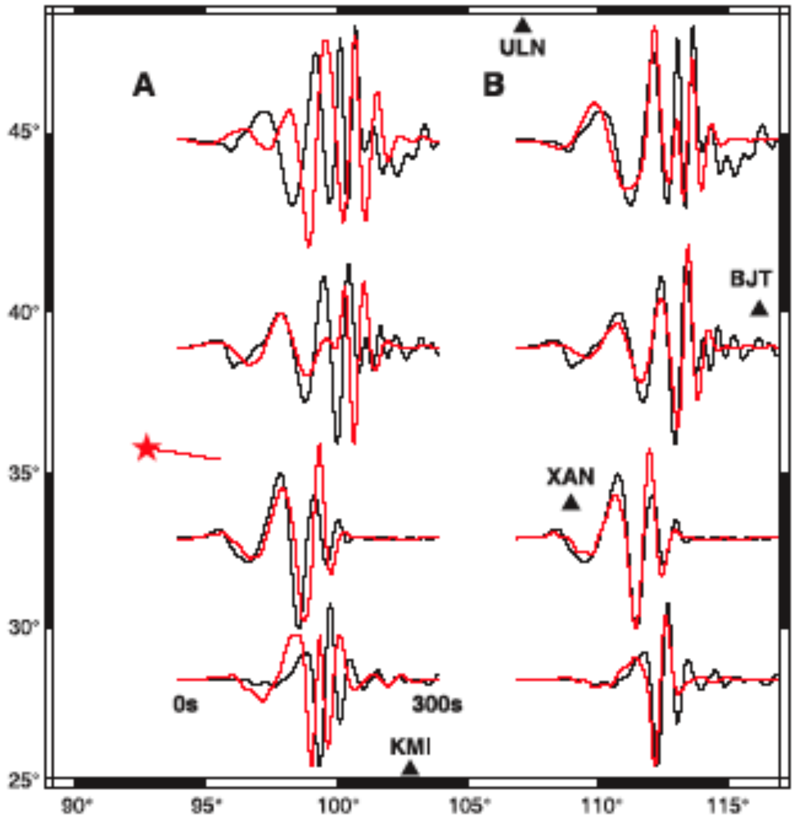

Fig. 1. Comparison between the recorded ground motion (in black) for the Kunlunshan earthquake and the one calculated (in red) for (**A**) a rupture velocity of 3 km/s and (**B**) the best-fitting rupture velocity, which averages 3.9 km/s. The component shown is the horizontal displacement in the direction transverse to the epicenter-station path; it starts with a reduced time equal to the epicentral distance divided by 4.5 km/s. The epicenter (star), the fault geometry (red line), and the station locations (triangles) are displayed.

Bouchon et al, Science 2003

1st segment : 2.8km/s
2nd and 3rd segment: 5km/s (supersonic for shear waves!)
4th segment: undetermined

MOTIVATION

Rupture speed: Mode II and III limits

Occurrence of supershear : **mode II only**

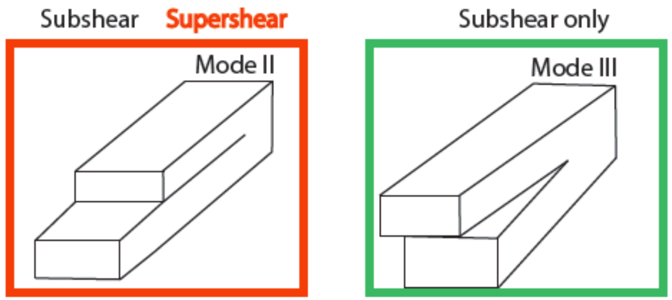

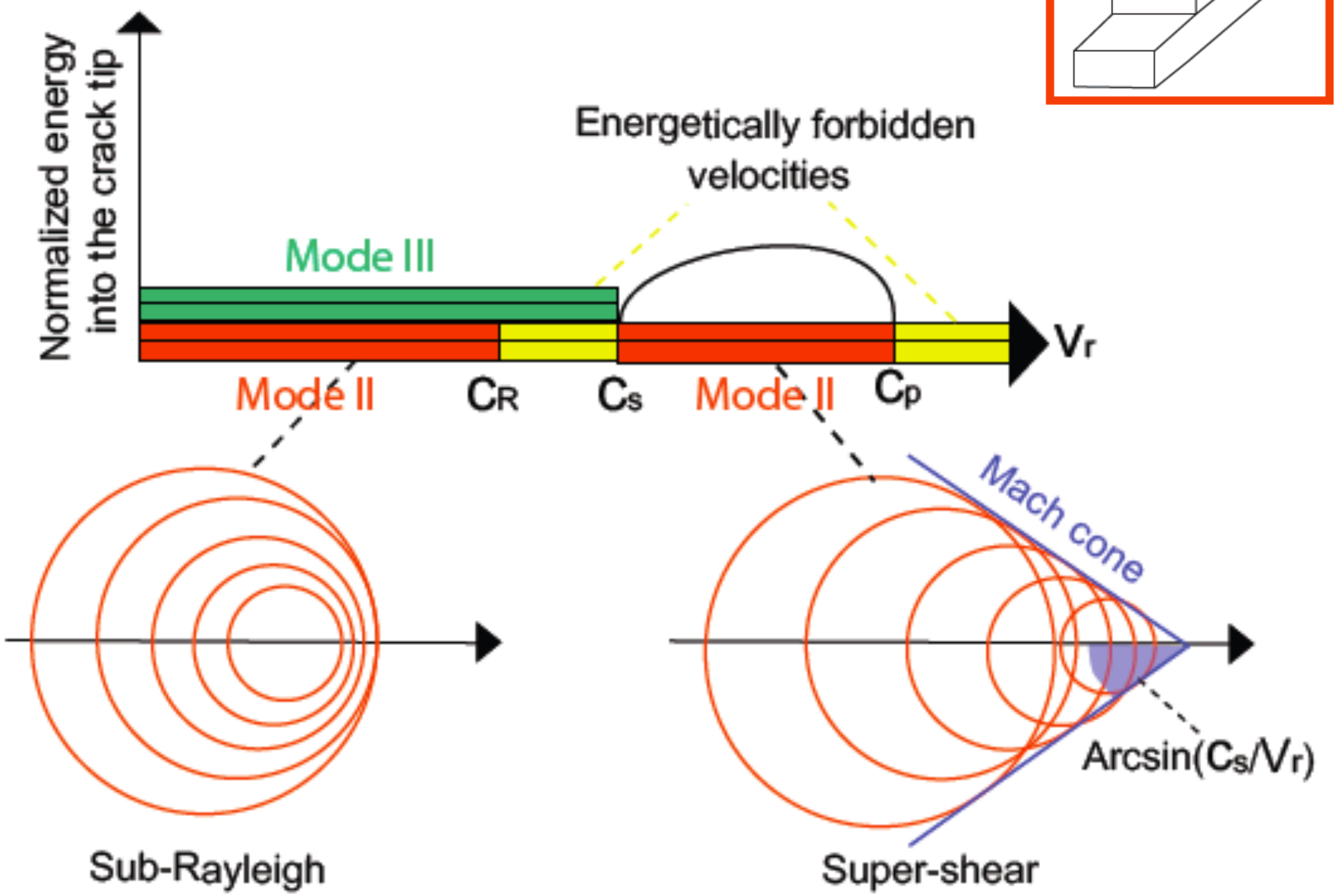

MOTIVATION

MOTIVATION

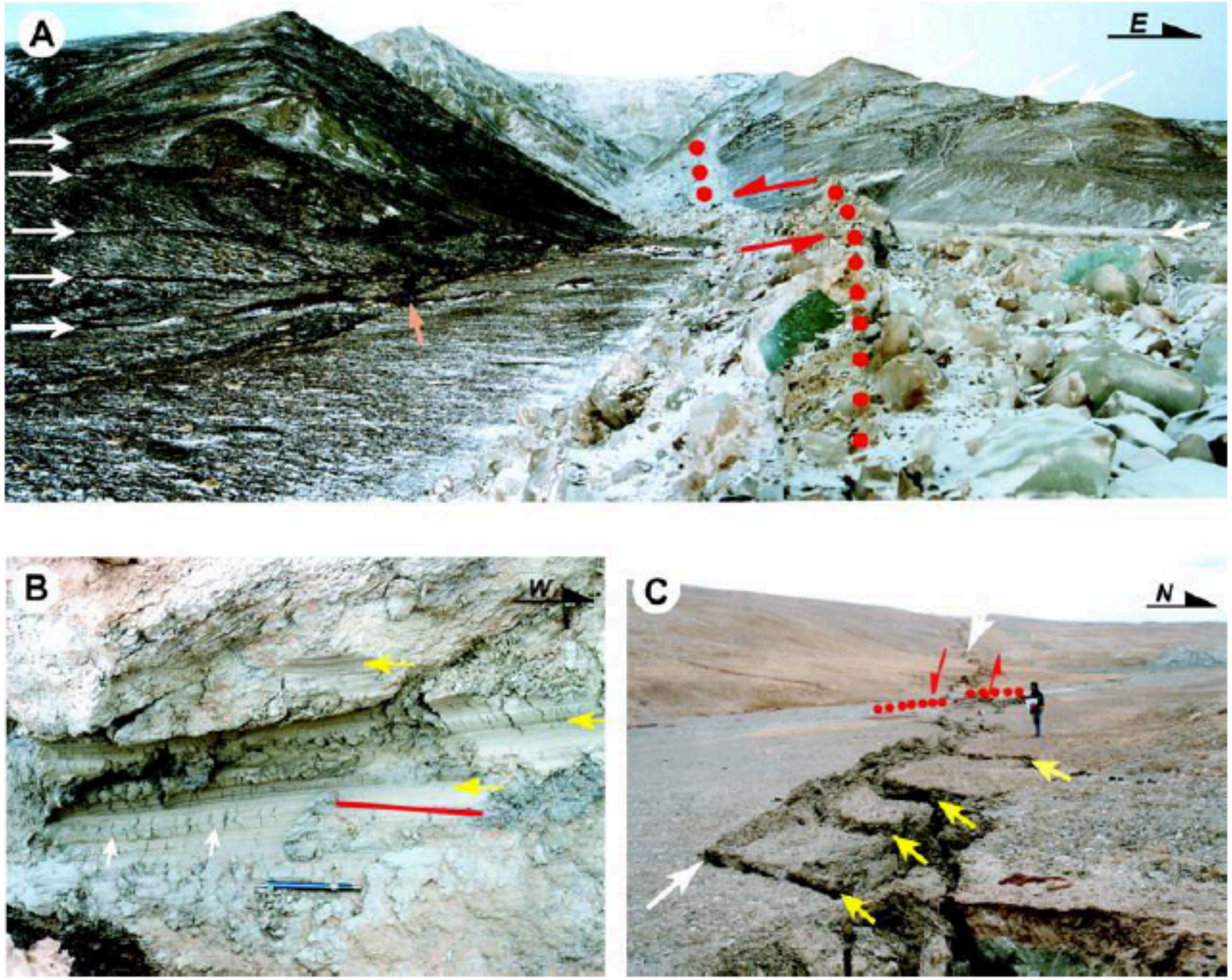

Kunlunshan earthquake: longest strike slip rupture ever observed

MOTIVATION

Only existing near-field record for Denali 2002, at Pump Station 10

A - pulse like super-shear rupture
(energetic Mach front)
B - Most probably Rayleigh waves
C - Trailing Rayleigh rupture propagation?

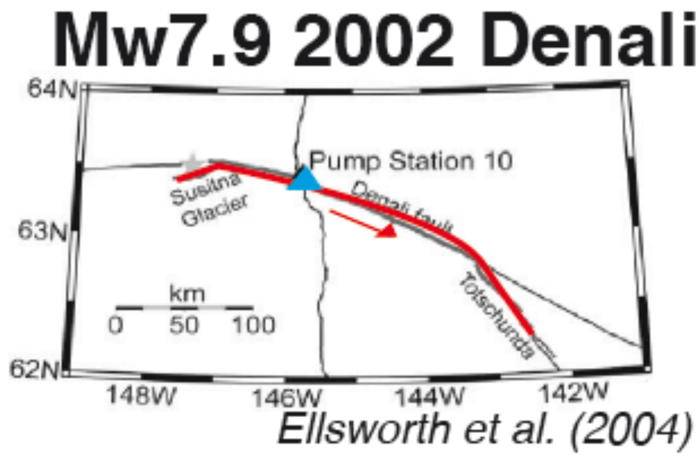

Fault Parralel velocity record at PS10

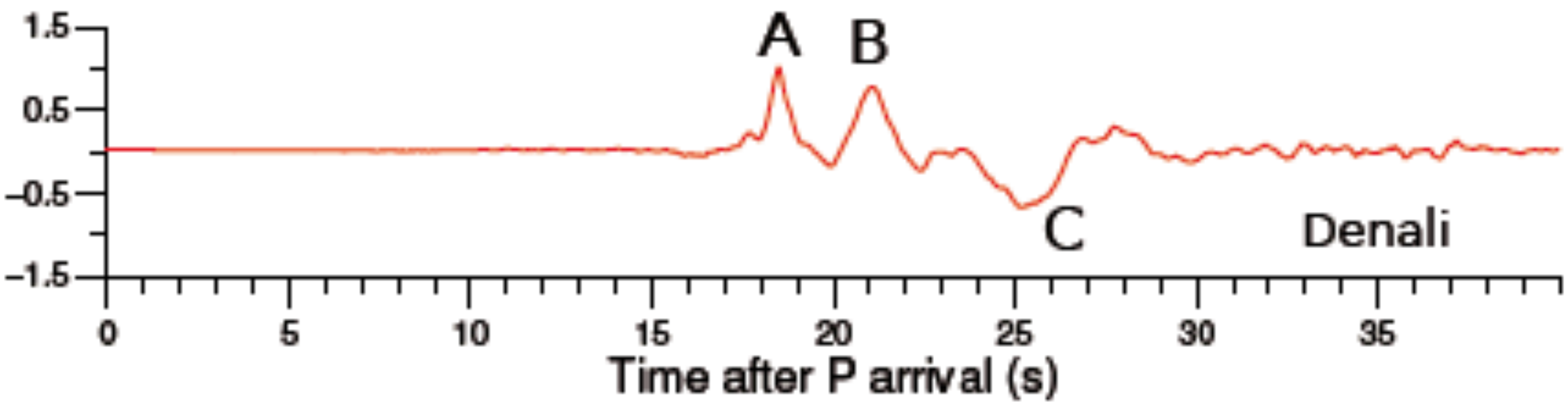

MOTIVATION

Subshear and supershear ruptures in birefringent polymers

Xia, Rosakis et al., Science 2004

Nielsen et al., GJI 2010

Schubnel et al. EPSL 2012

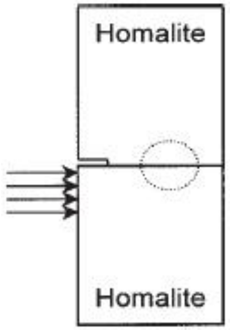

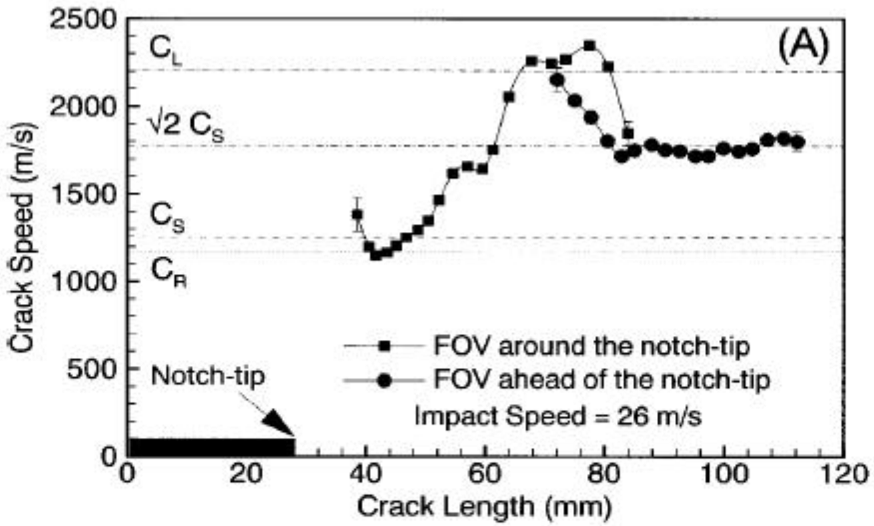

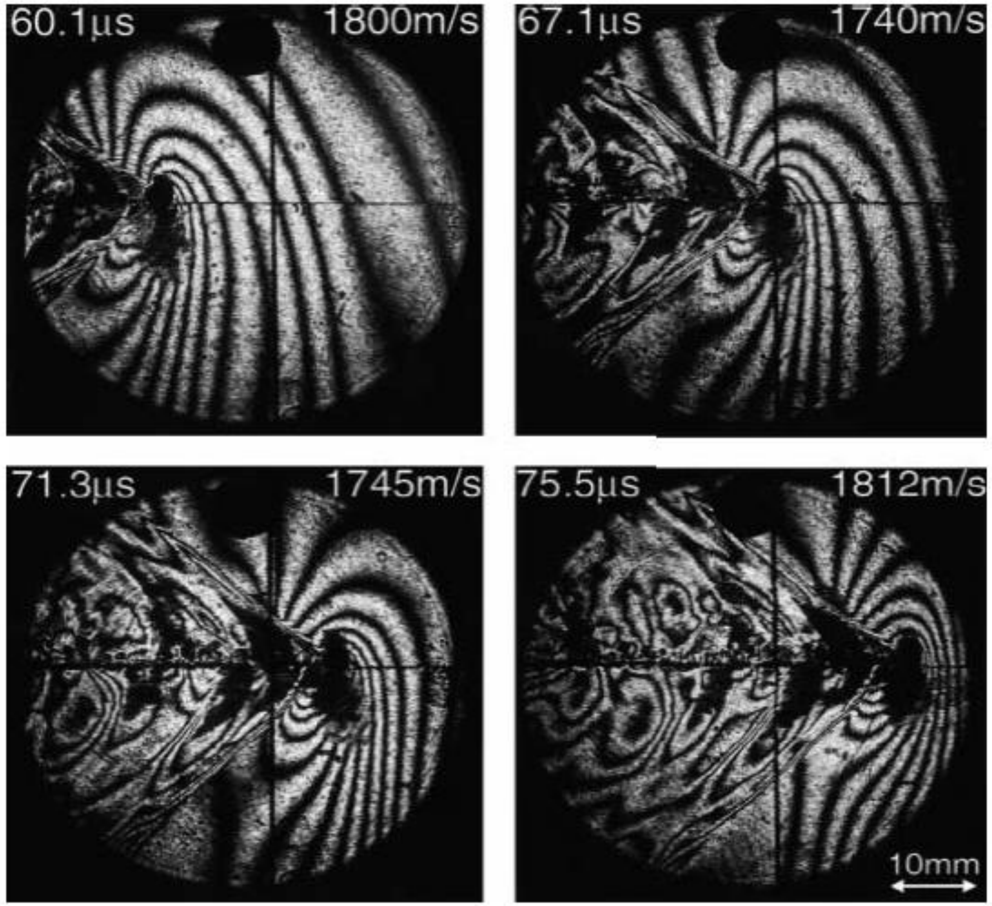

Reproducing depth in the lab

(01) Triaxial apparatus - 100MPa/200°C

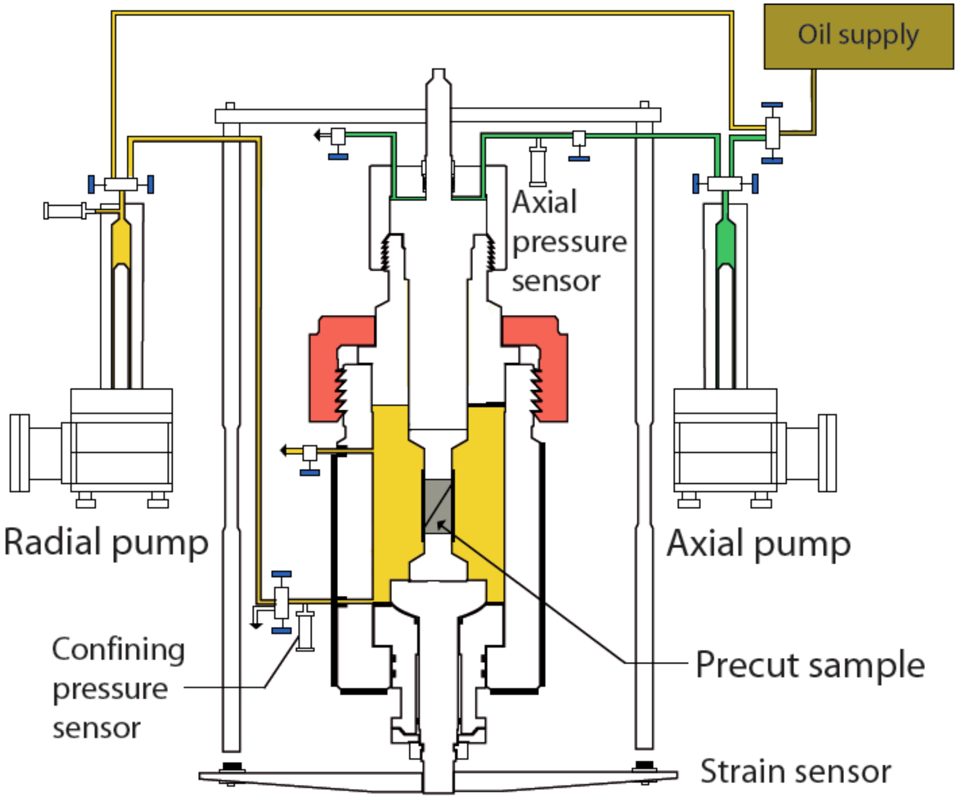

Scheme of the triaxial apparatus of the ENS

- Designed specially for acoustics
- Corrosive fluids injection (pH<3) in gas, water or supercritical phase
- Up to 100MPa confinement and pore pressure, 70 tons axial load

Reproducing depth in the lab

(02) Acoustic Recorder – 16 channels

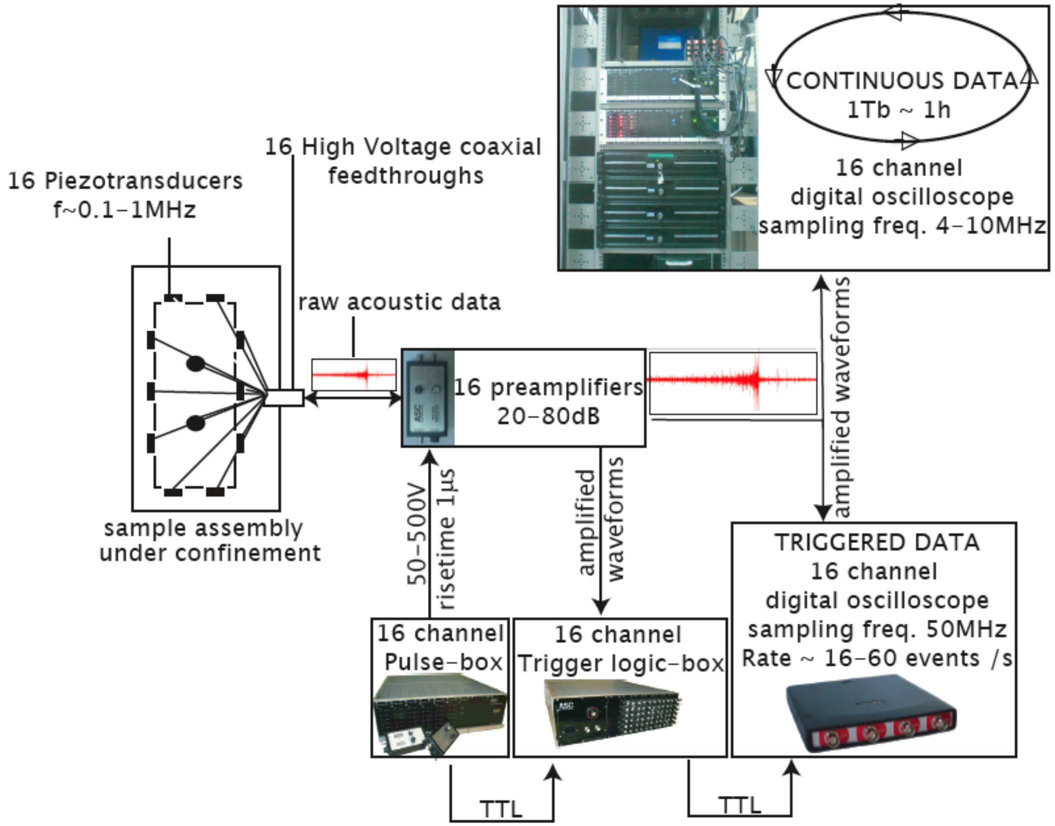

- Continuous acoustic wfms recorded using Richter minisystem (ASC Ltd., 4 MHz sampling freq. on 16 channels)
- Triggered data - up to 16 events/ sec
- Each transducer can be used as source for velocity measures (P&S)

Rupture speeds…

INTACT SAMPLE of Fontainebleau sandstone

Nucleation zone (~1cm^3)

Quasi static to dynamic @ >mm/s)

Terminal speeds ~ 10m/s

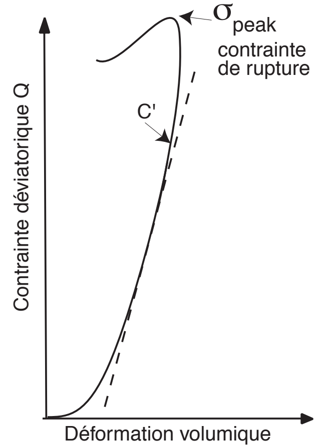

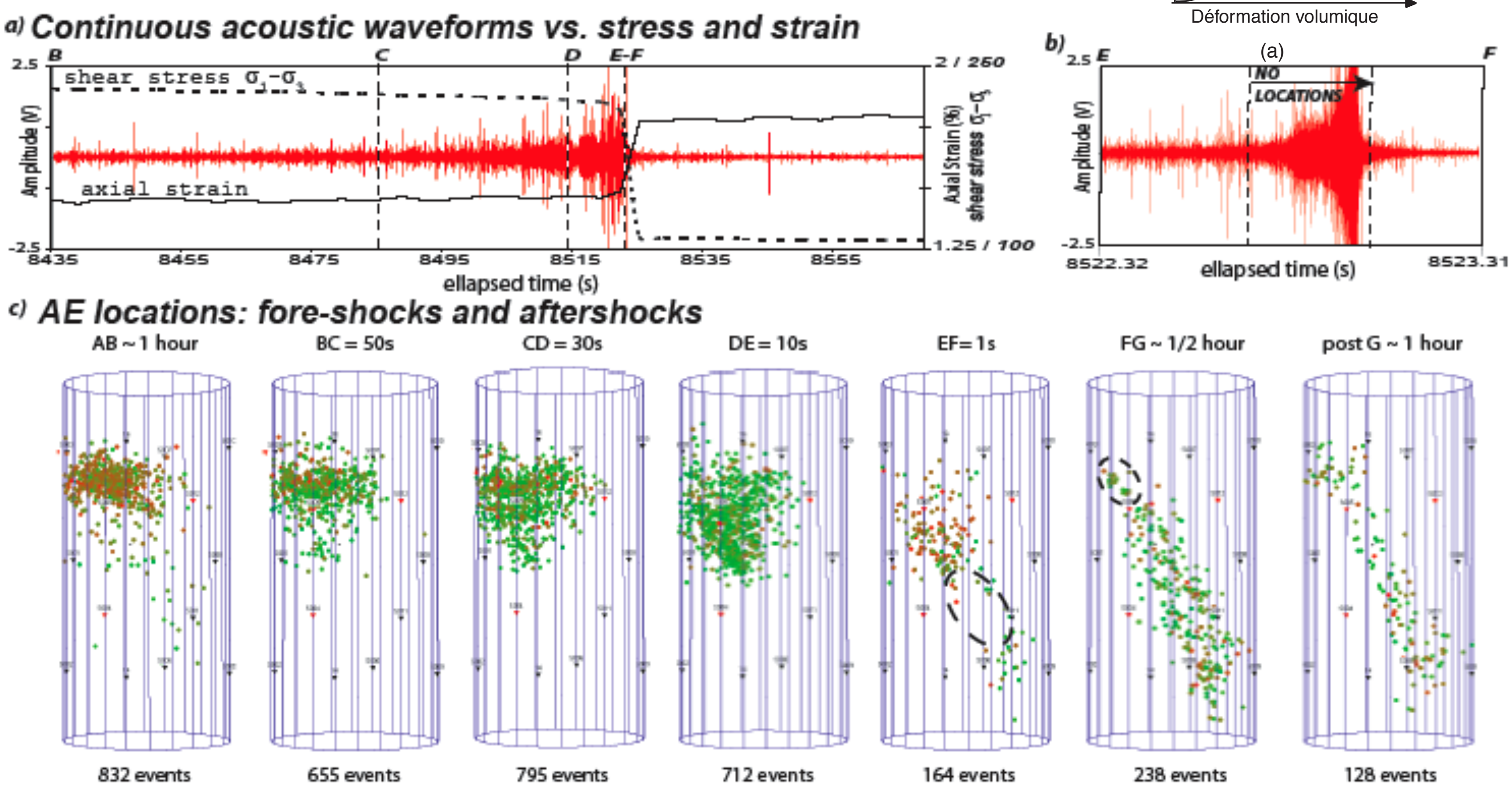

Schubnel et al., 2007

Rupture speeds…

Nucleation and fracture growth in **INTACT SAMPLE** of Westerly granite

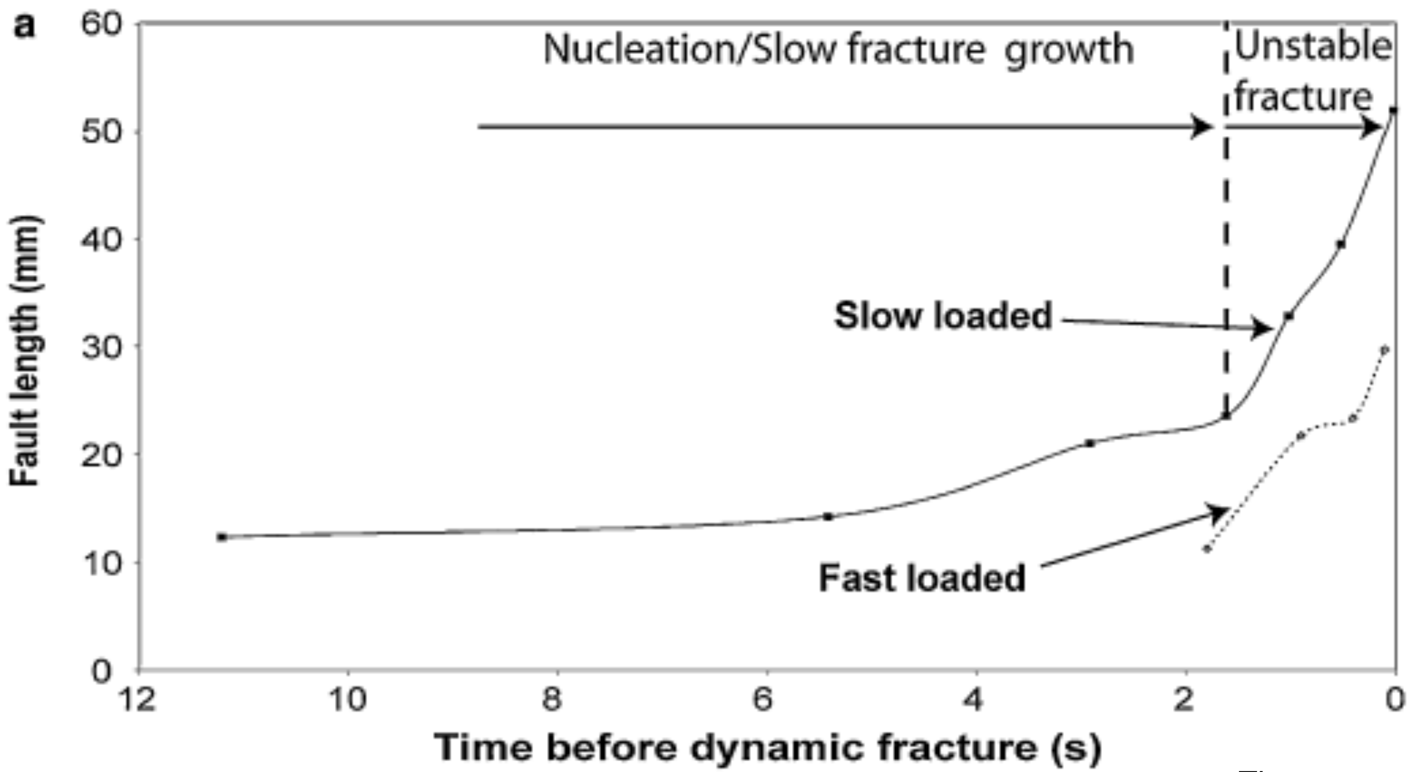

Thompson et al. 2006

Stick-Slip Events (SSE) as an EQ analogue

Pc < 300MPa 10^{-4} > strain rate > 10^{-5}

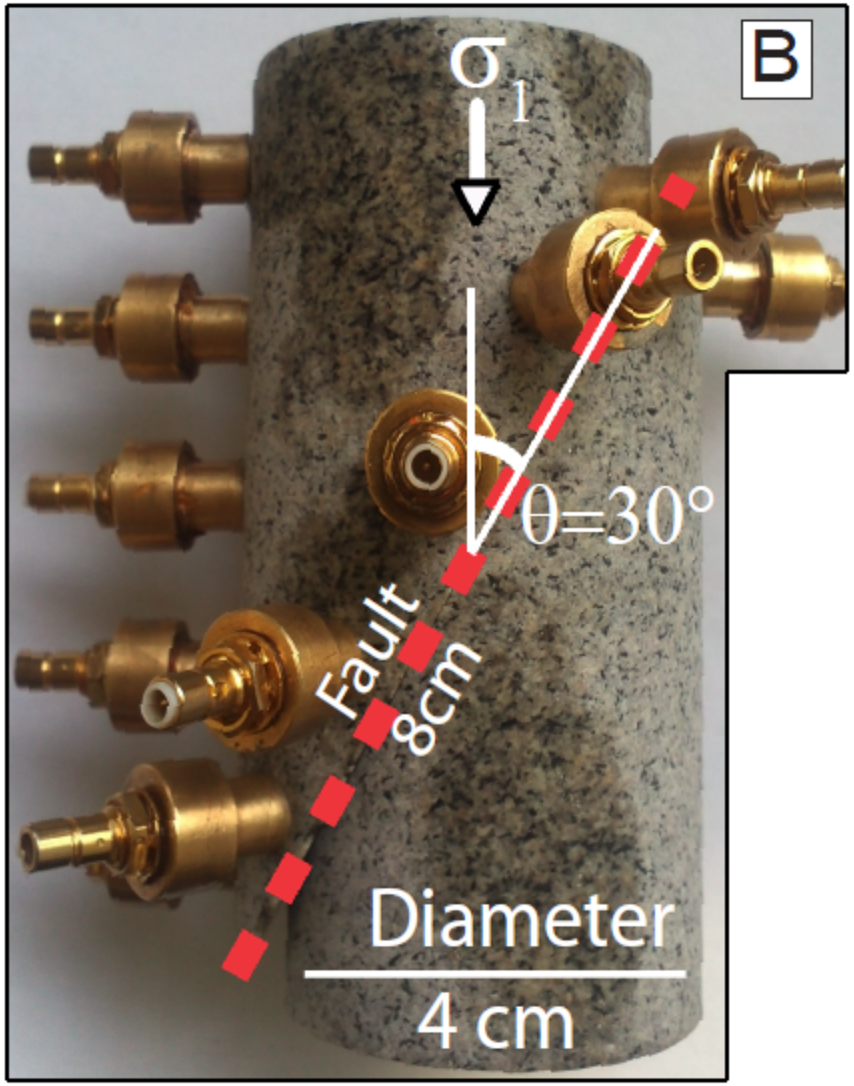

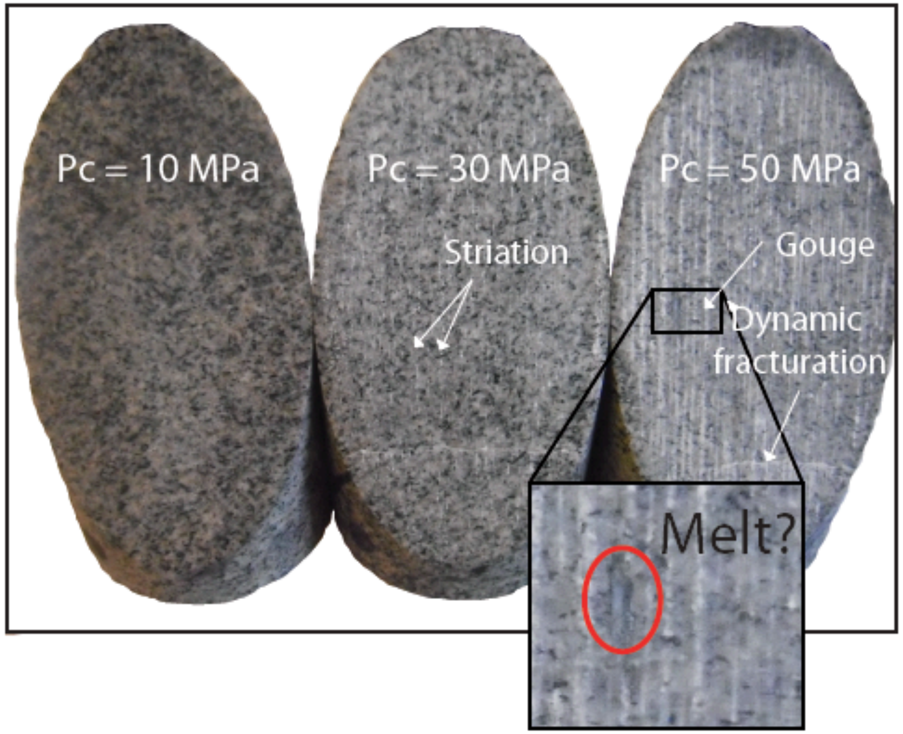

Photographs of fault surfaces after experiments

Stick-Slip Events (SSE) as an EQ analogue

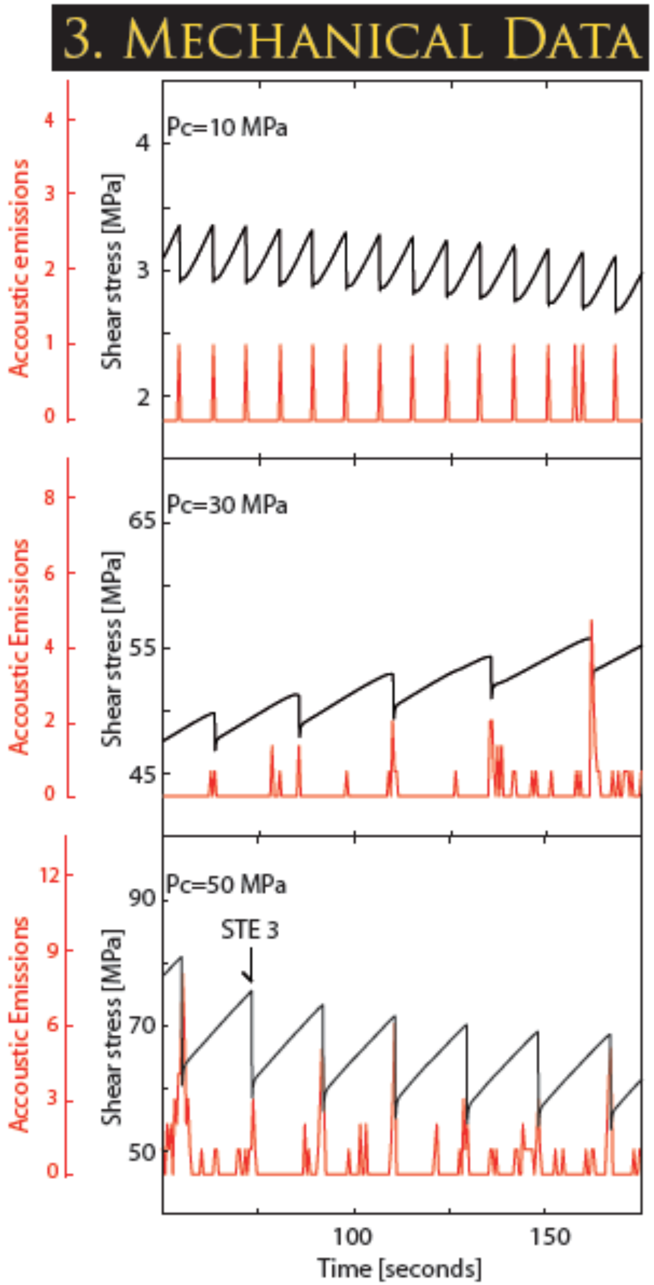

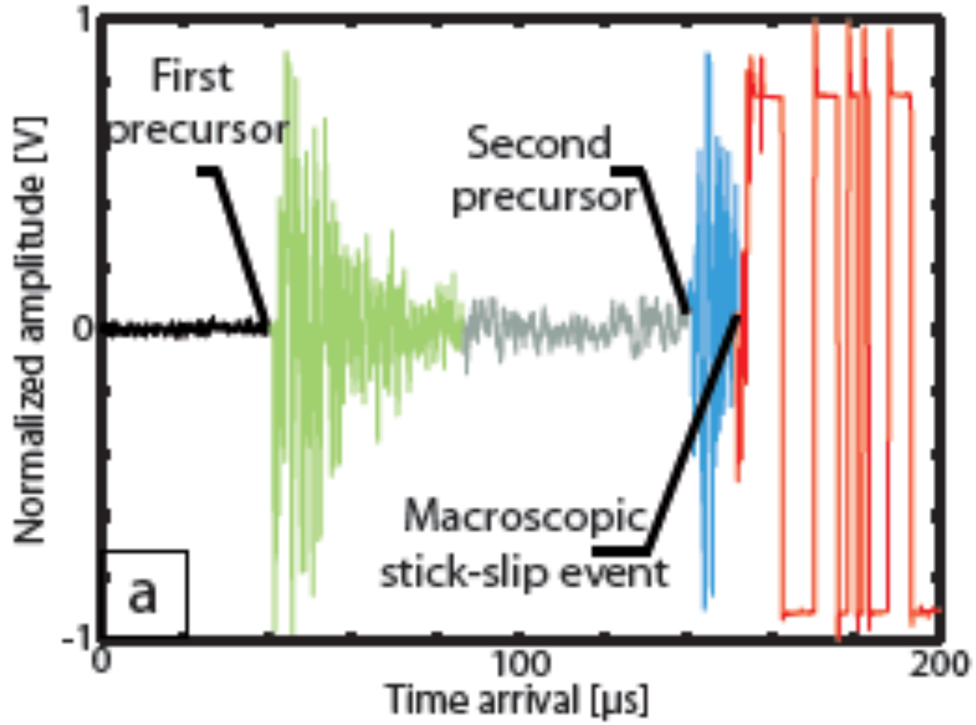

CFMR, Arts et Métiers, Février 2013

Measuring the rupture speed

V_r estimated using arrival time of the rupture front passing by each sensor

Calculation of the theoretical arrival time on each sensor for
(i) nucleation point on the fault plane
(ii) different initiation times
(iii) different rupture front geometry

$$t^{th} = f(Vr, To, x, y)$$

Least square function between experimental and theoretical arrivals time

$$\min\left[\frac{\sum_N (dt^d - dt^{th})^2}{N}\right] => (x, y, To, Vr)$$

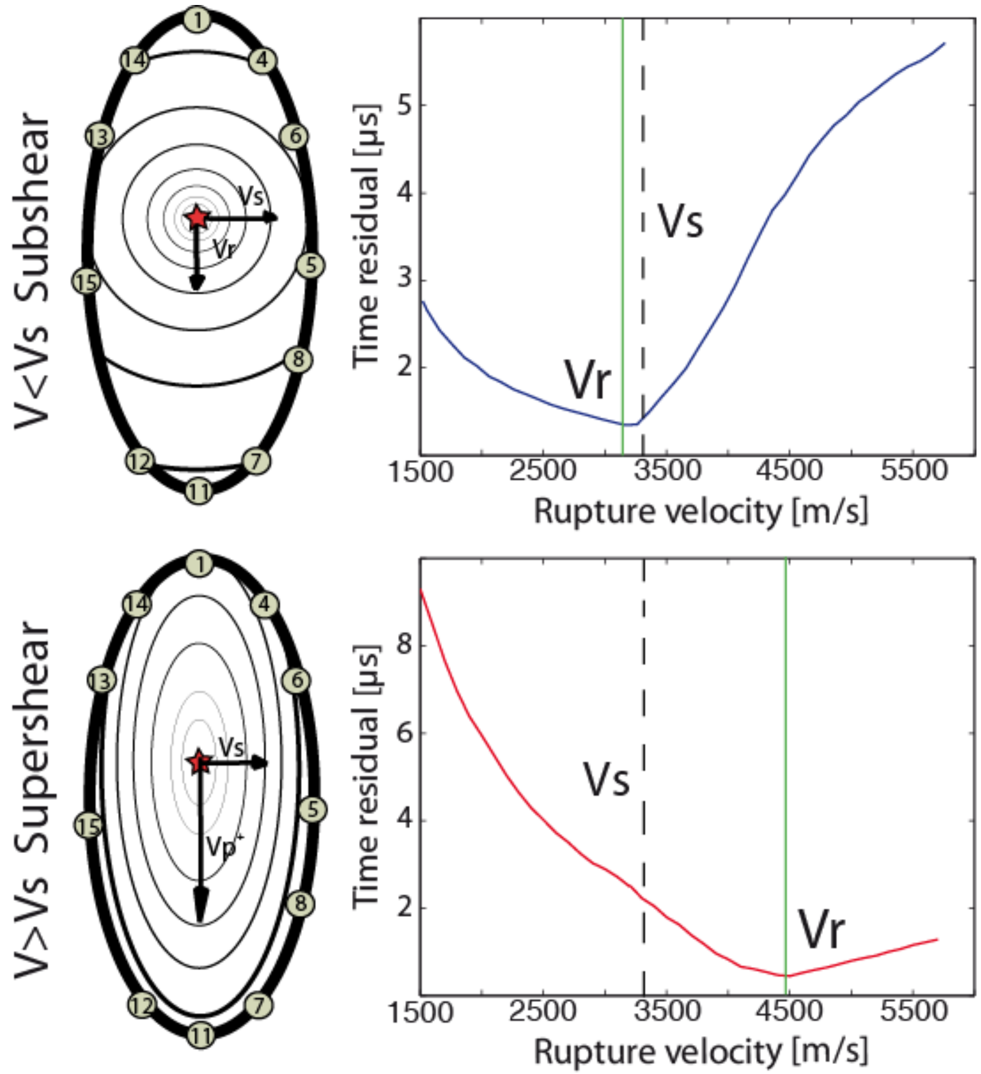

Sub-Rayleigh rupture during SSE

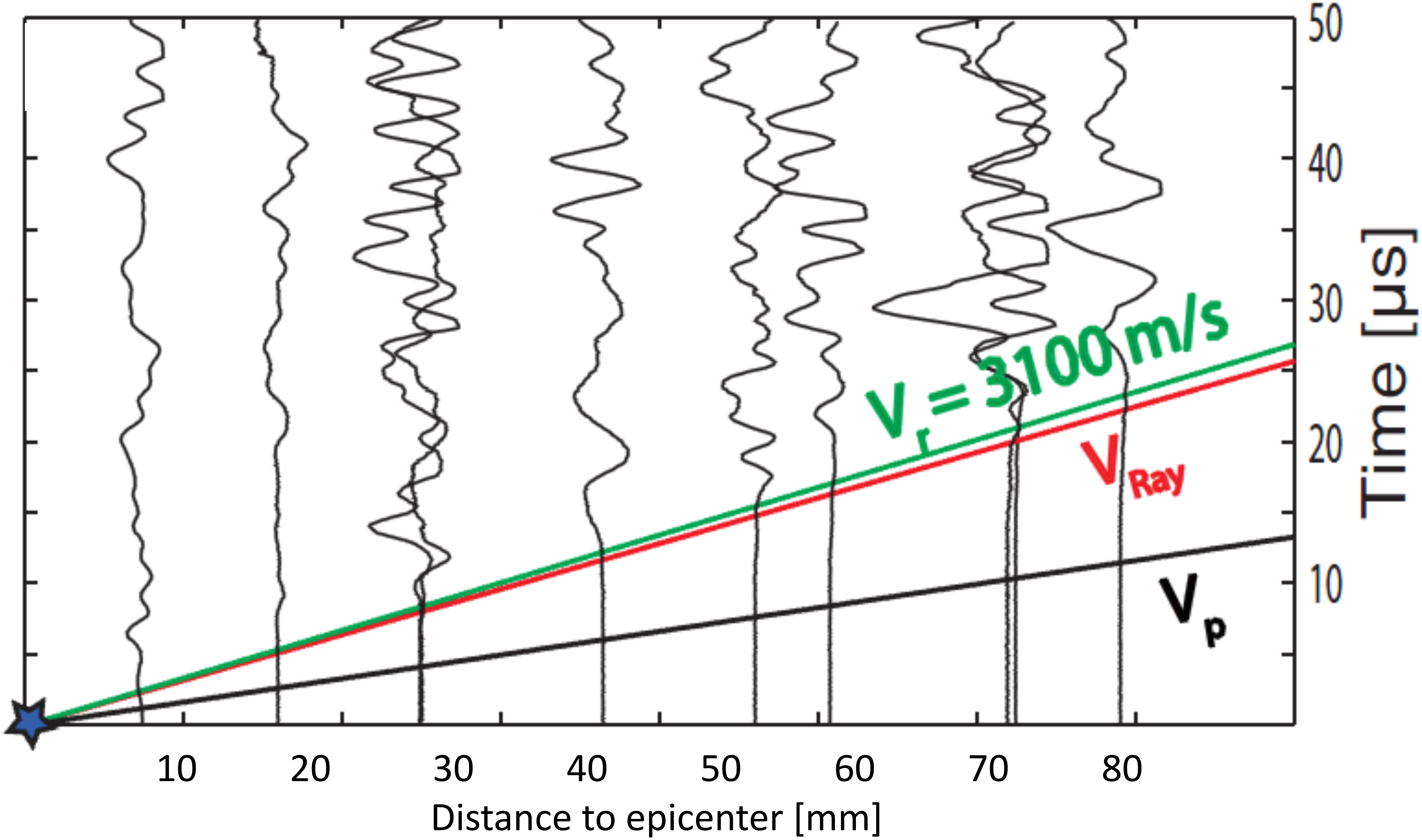

Supershear rupture during SSE

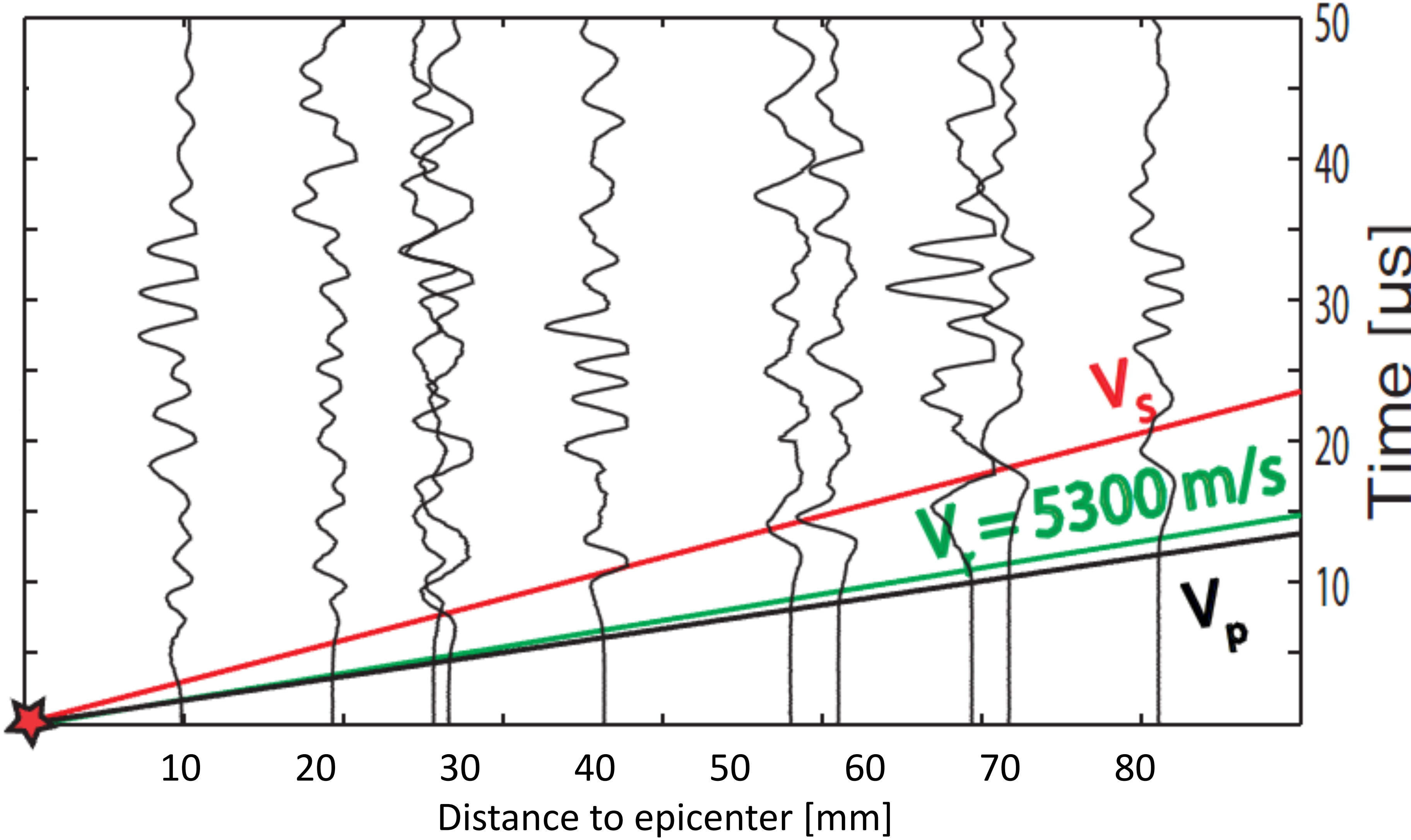

Supershear rupture during SSE

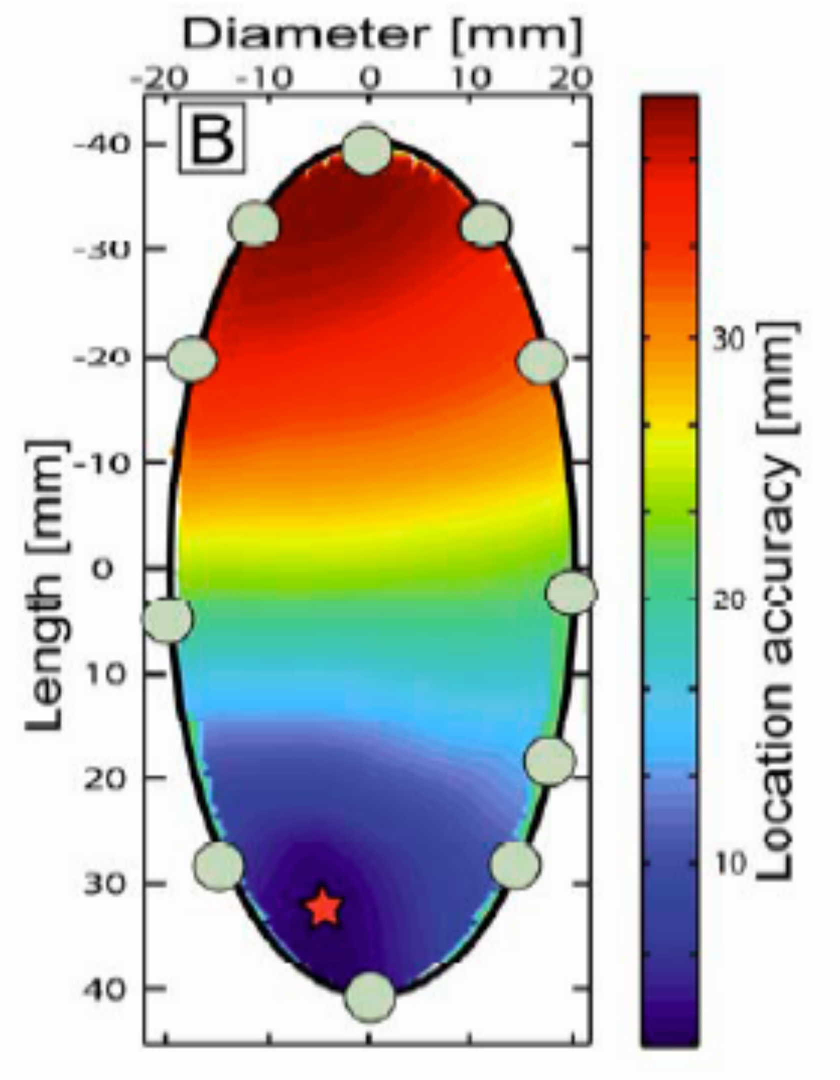

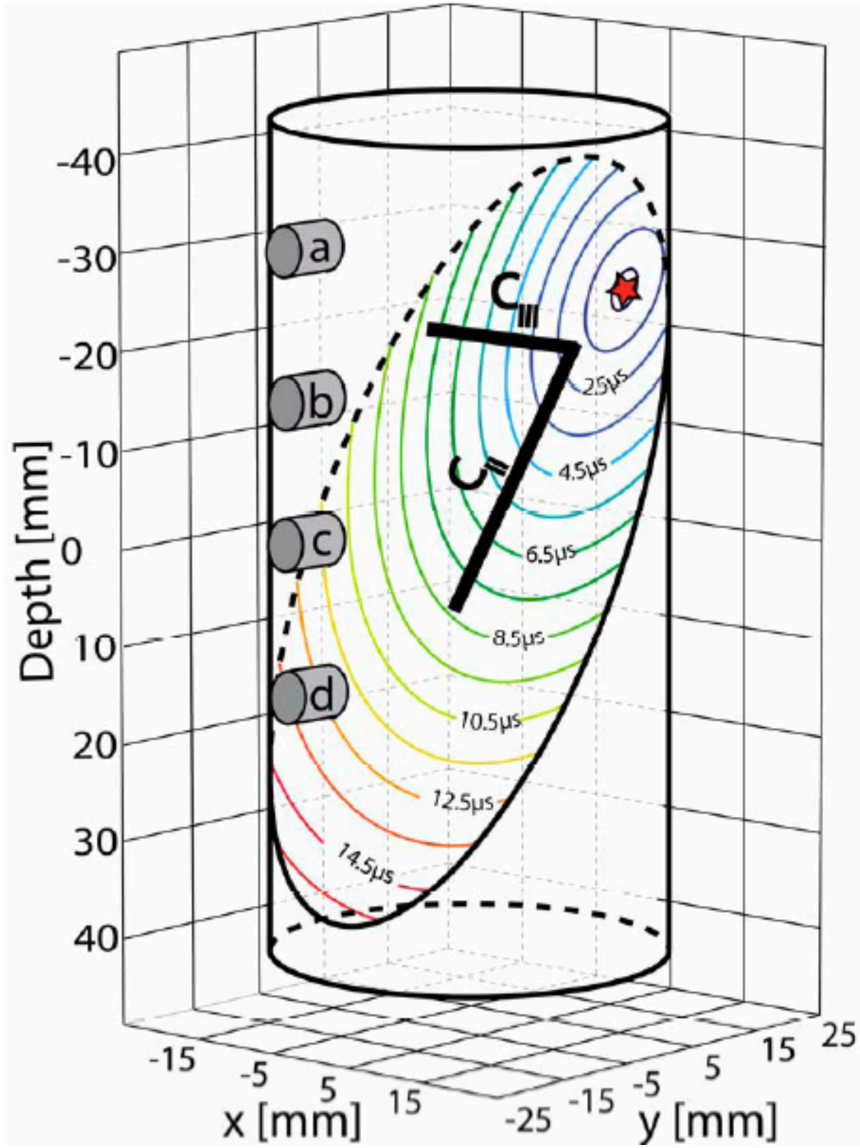

Mach Front arrival

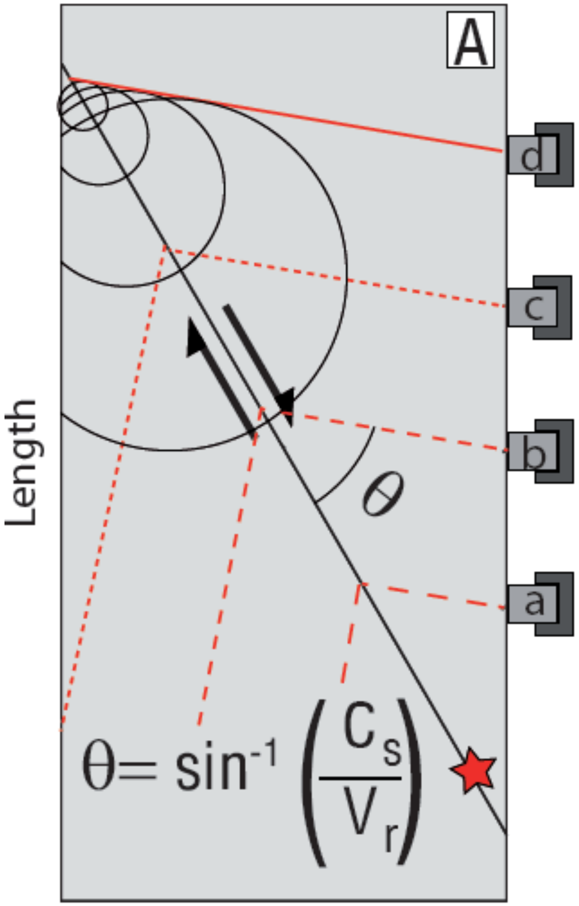

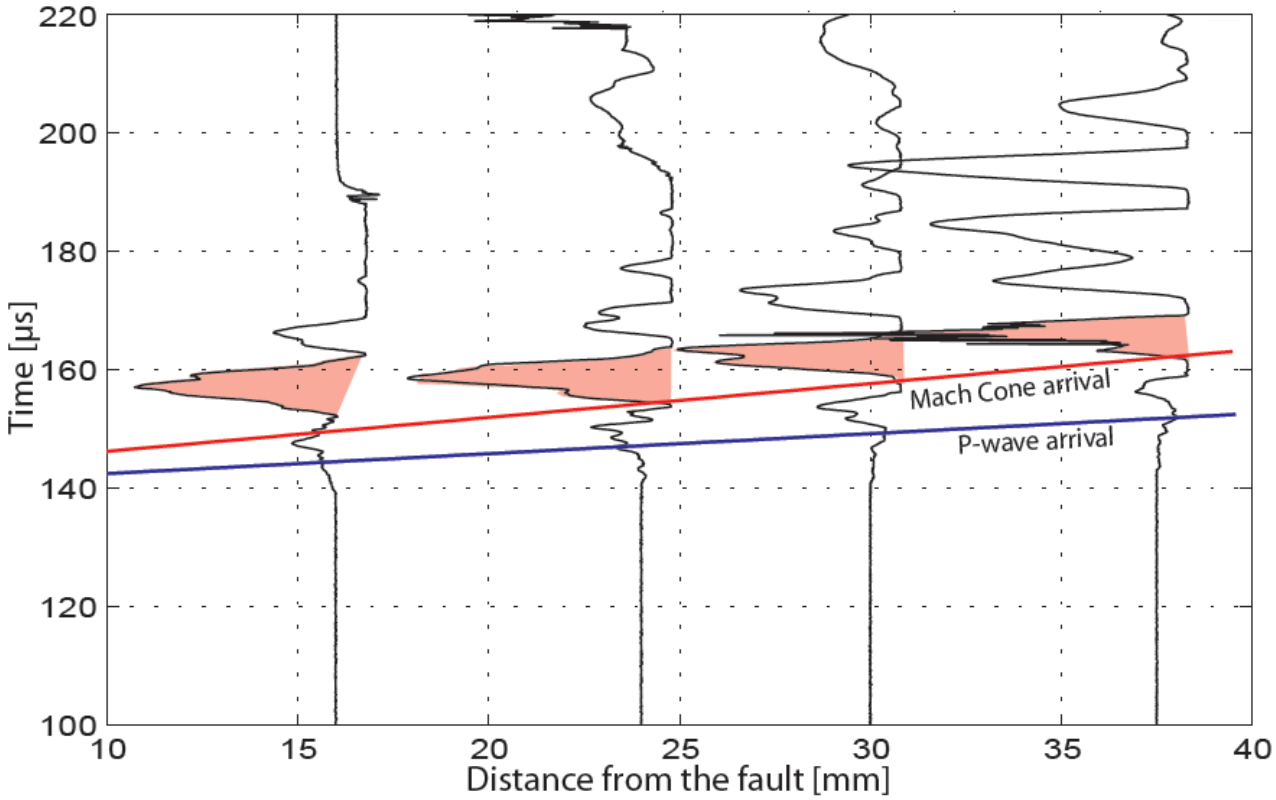

First clear laboratory evidence of supershear rupture in rocks!

CFMR, Arts et Métiers, Février 2013

Comparison with synthetics

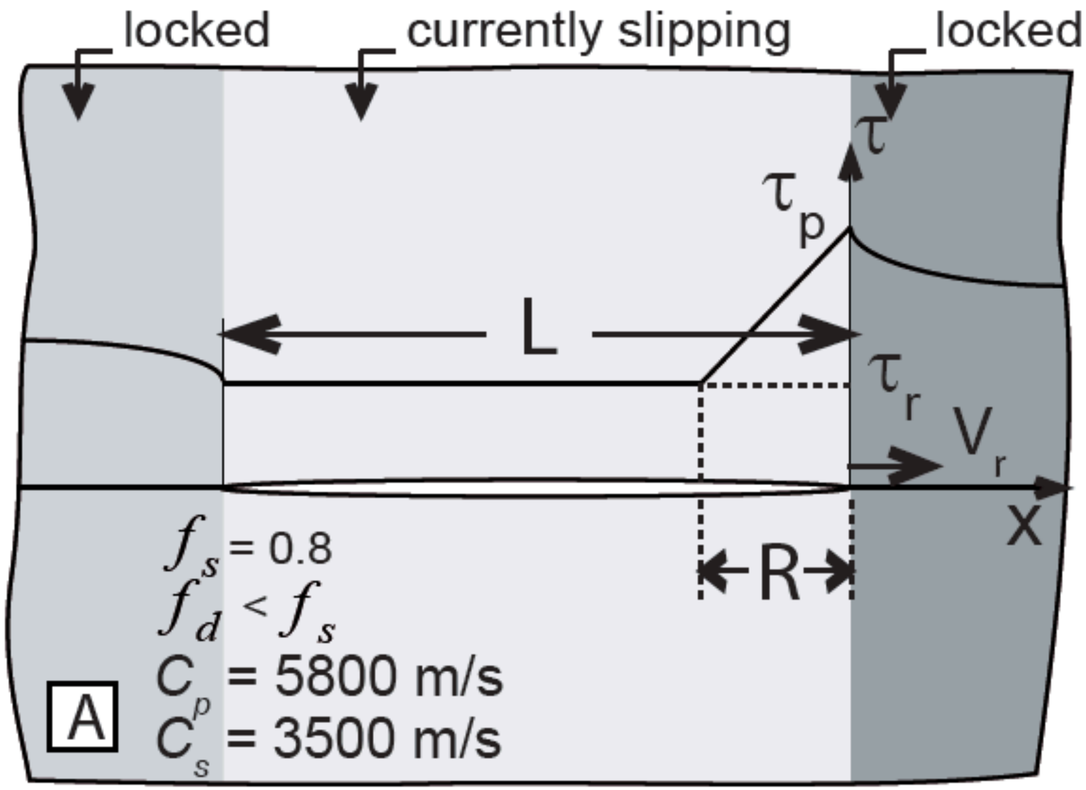

2D steady state
slip pulse model
(Dunham and Archuleta, 2005)

$$\dot{u}\left(\frac{x}{L},\frac{y}{L}\right) = \frac{(f_s - f_d)(-\sigma^0_{yy})C_s}{\mu}\boldsymbol{\Omega}\left(\frac{x}{L},\frac{y}{L},\frac{R}{L},\frac{V_r}{C_s}\right)$$

Comparison with synthetics

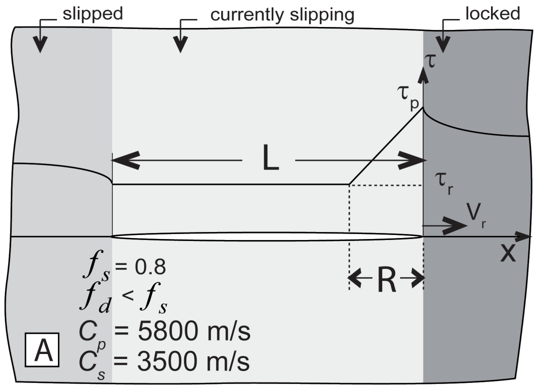

2D steady state
slip pulse model
(Dunham and Archuleta, 2005)

Sub-Rayleigh

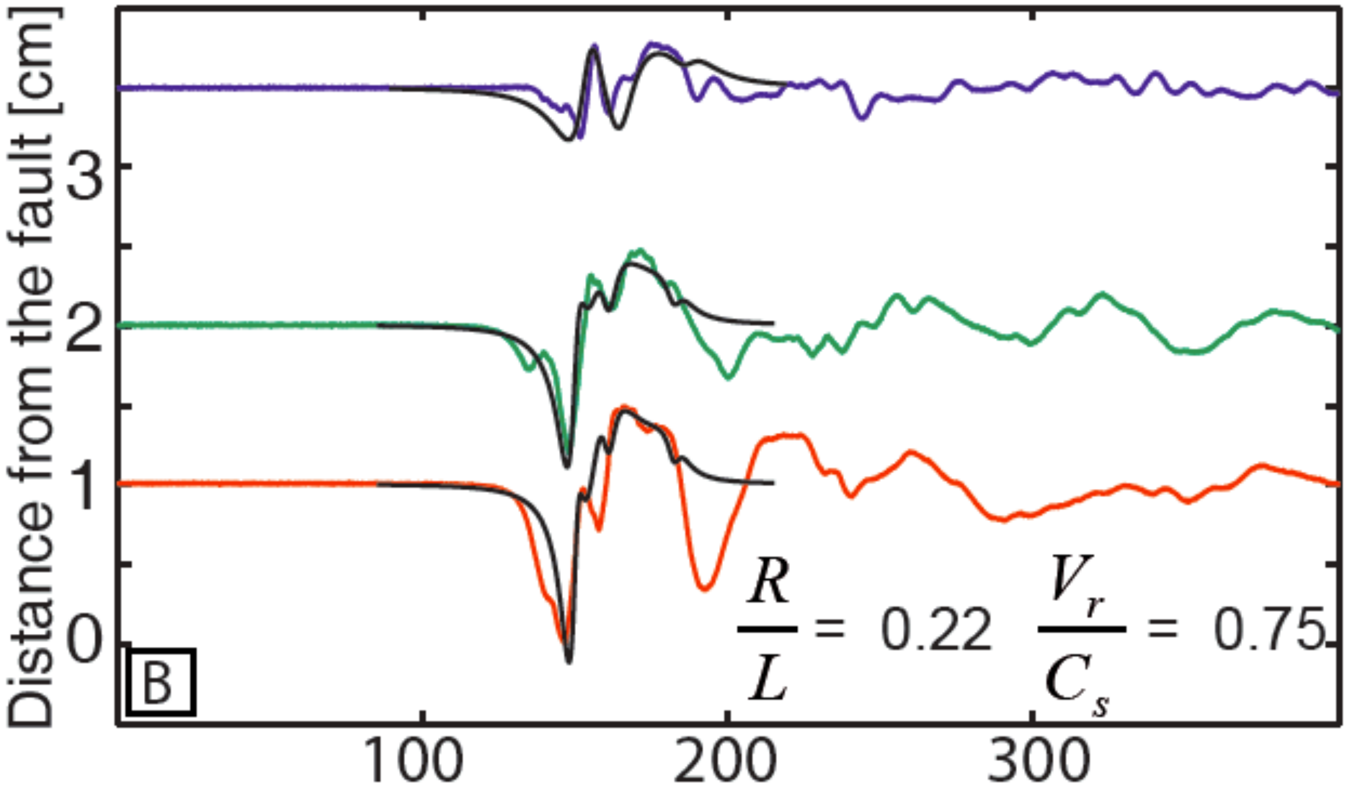

Comparison with synthetics

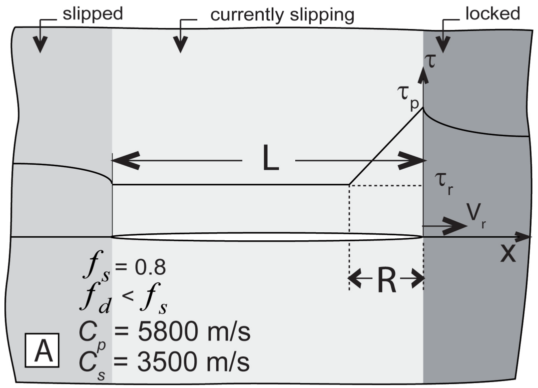

2D steady state
slip pulse model
(Dunham and Archuleta, 2005)

Effect of rupture velocity

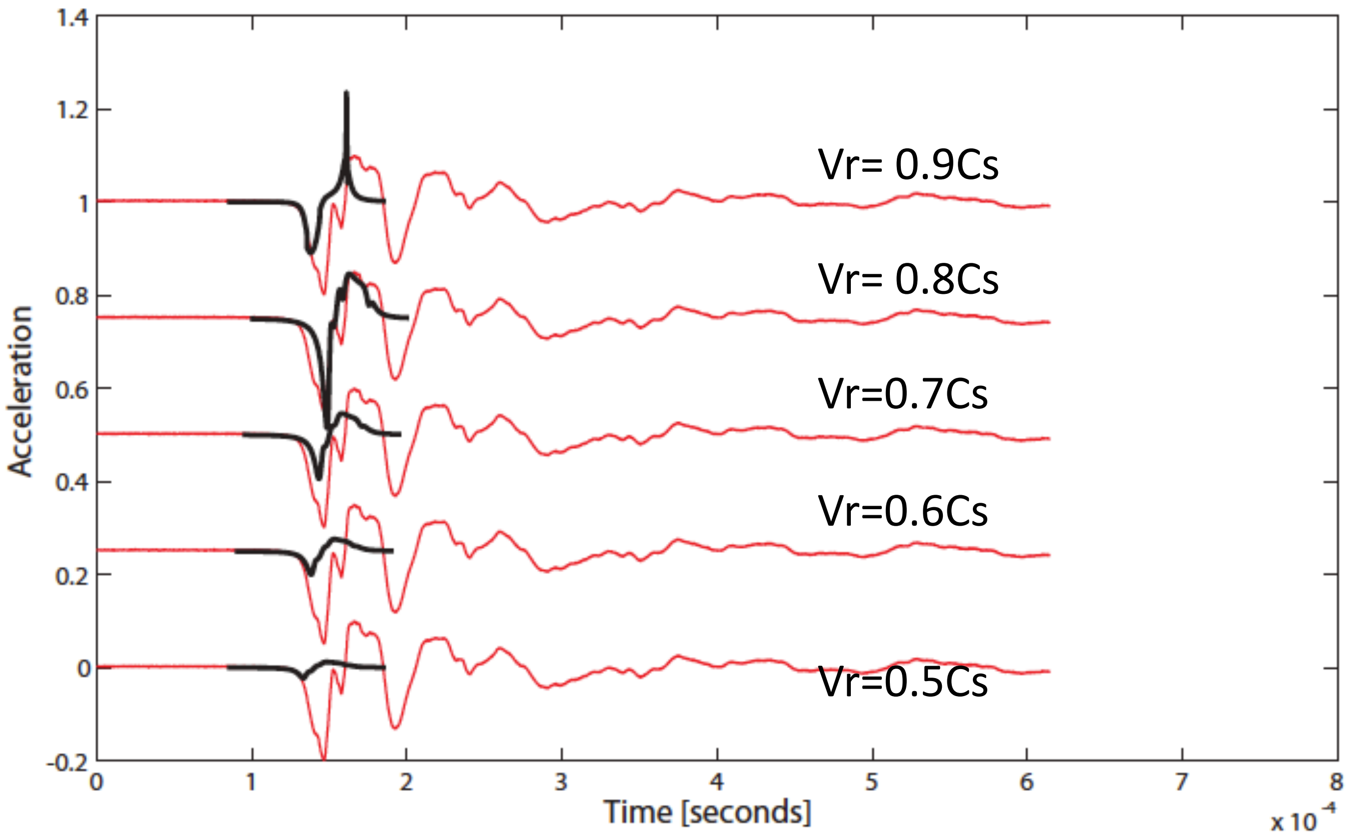

Comparison with synthetics

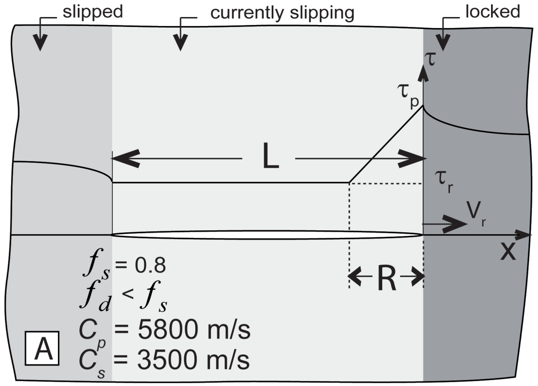

2D steady state
slip pulse model
(Dunham and Archuleta, 2005)

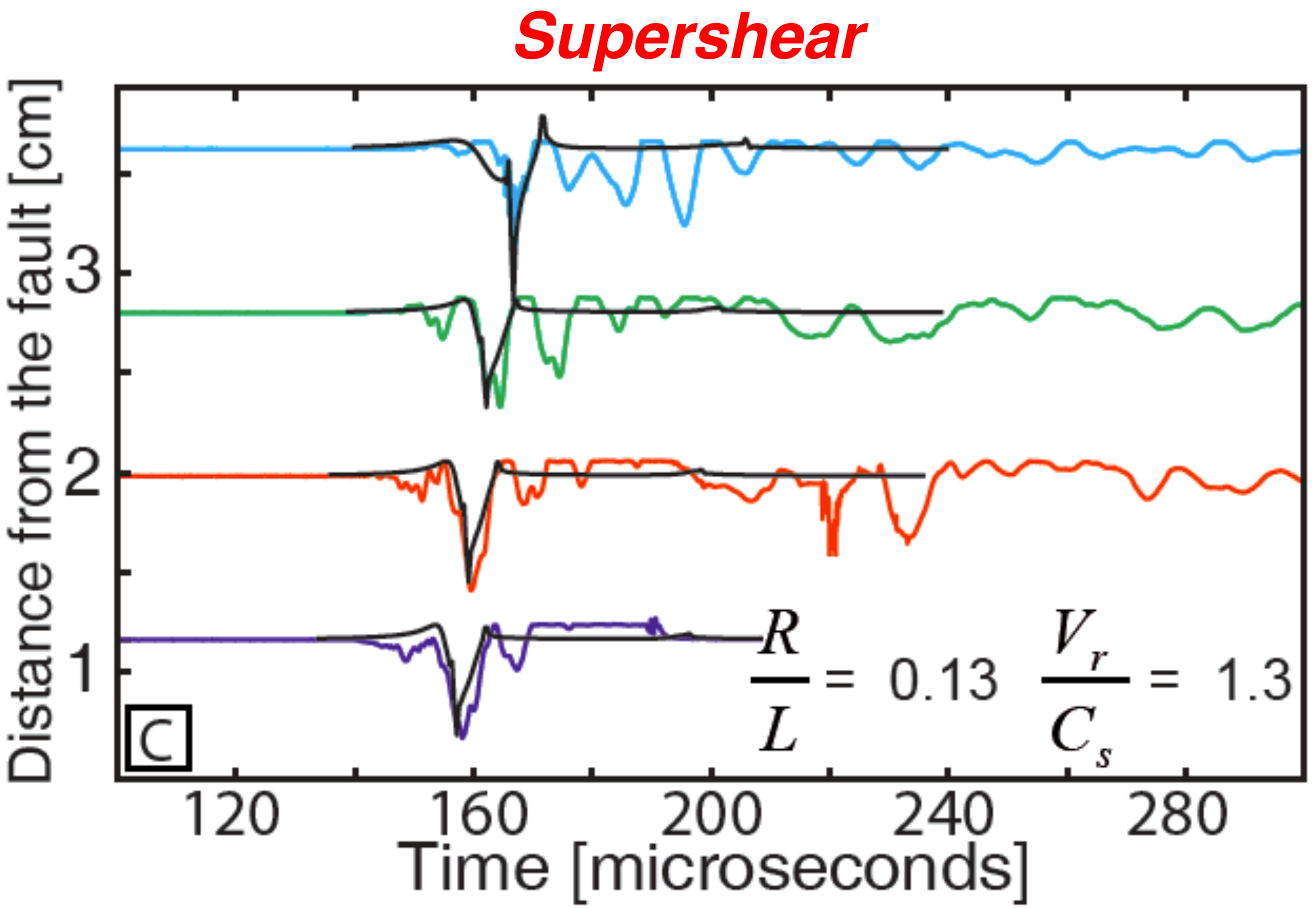

Transition length

Supershear rupture if the transitional length **L is** smaller than $\mathbf{L_f}$

Estimation using a semi-empirical law:

Andrews, 1976
Xia et al., 2004

$$L = \frac{39.2}{\pi(1-\nu)} \frac{1}{(1.77-S)^3} \frac{G\mu}{((f_s - f_d)\sigma_n)^2}$$

Where S is the Seismic Ratio

$$S = (\tau_p - \tau_0)/(\tau_0 - \tau_r)$$

G is the fracture energy
τ_0 is the initial shear stress
τ_r is the residual shear strength
τ_p is the peak strength

ν=0.25 Poisson ratio; μ=24GPa shear modulus

Transition length

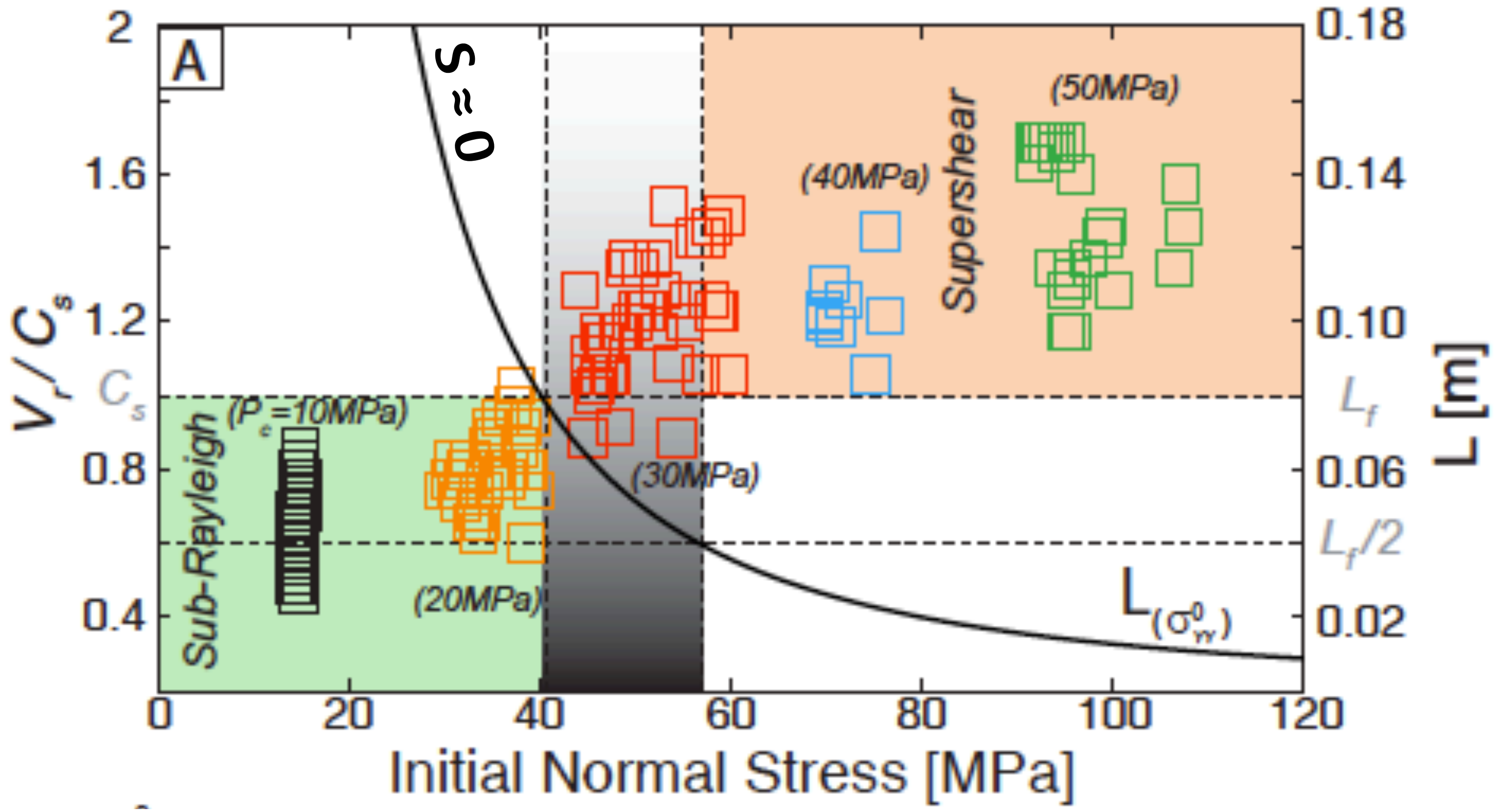

Stress drops

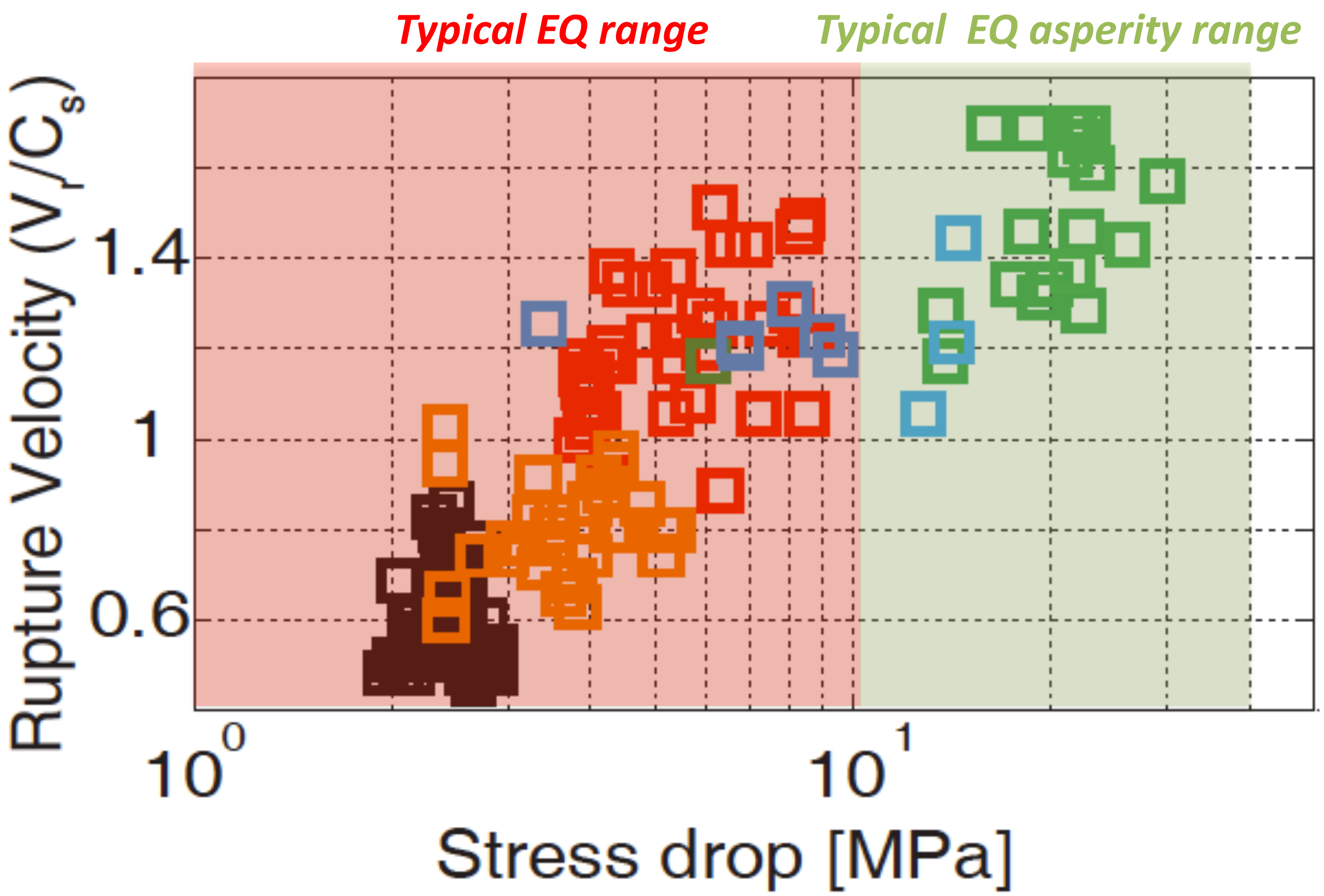

Frictional Heat: the mineral coupling

(for a crack-like rupture, 0.1 mm thickness)

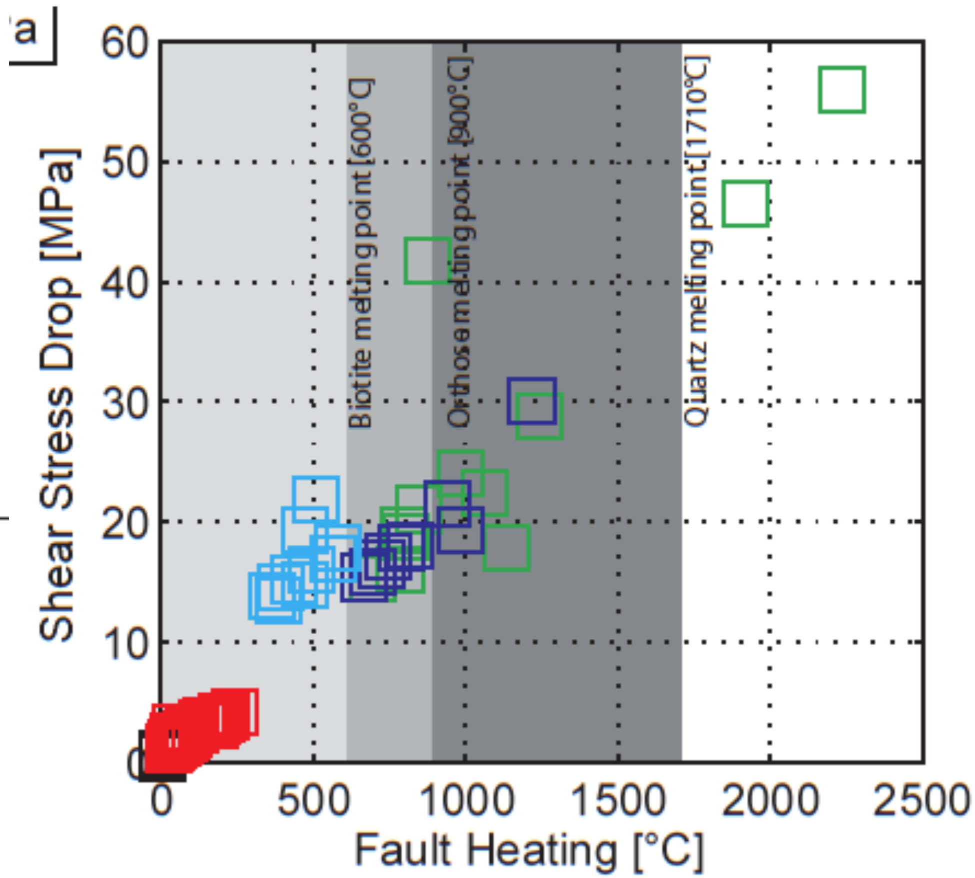

Xrd of fault gouge particles

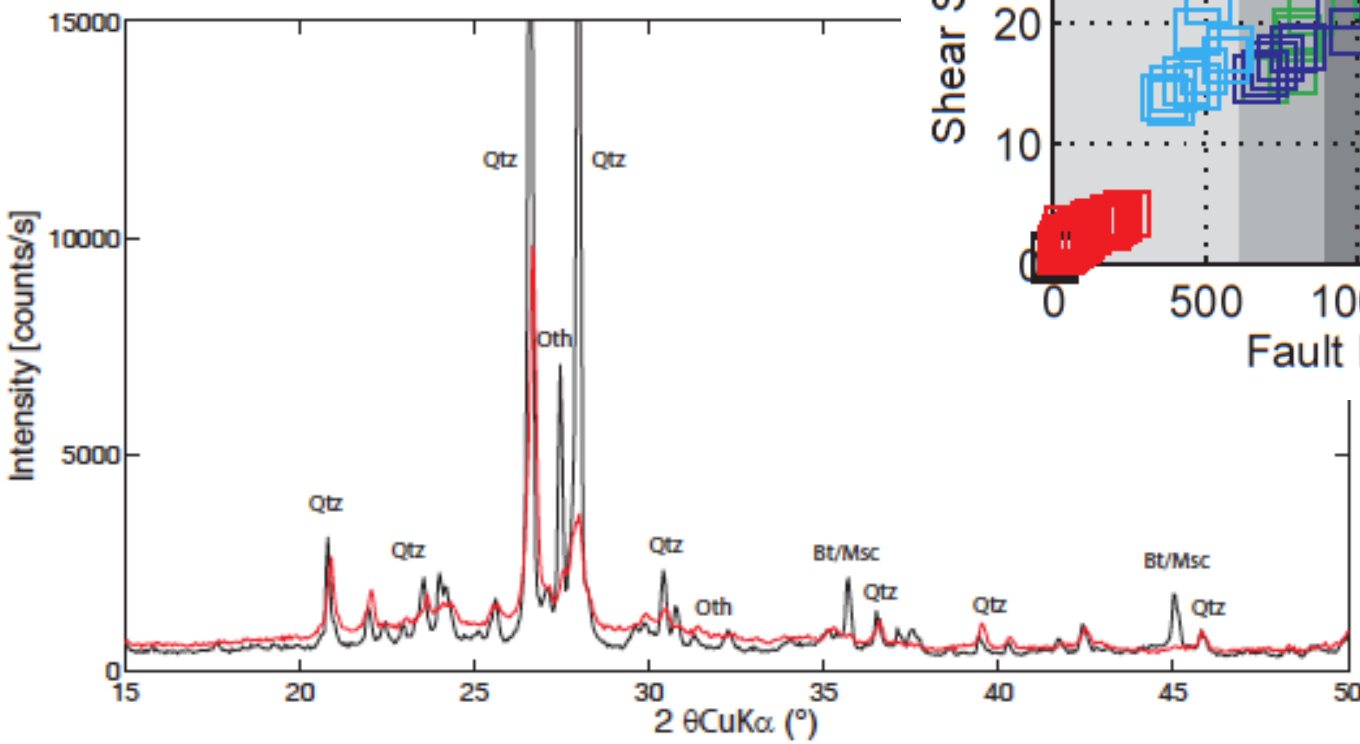

CONCLUSIONS

• SS ruptures can be spontaneously reproduced on saw cut samples in rocks, because the transition length to SS, in upper crustal conditions, is a few cm only. So what slows down rupture? Geometrical effects, roughness, gouge, etc…?

• Nevertheless, SS ruptures observed for 2MPa stress drops only, indicates that asperities might punctually break in SS during EQ prop, while overall rupture SR. Importance consequence for EQ HF radiation.

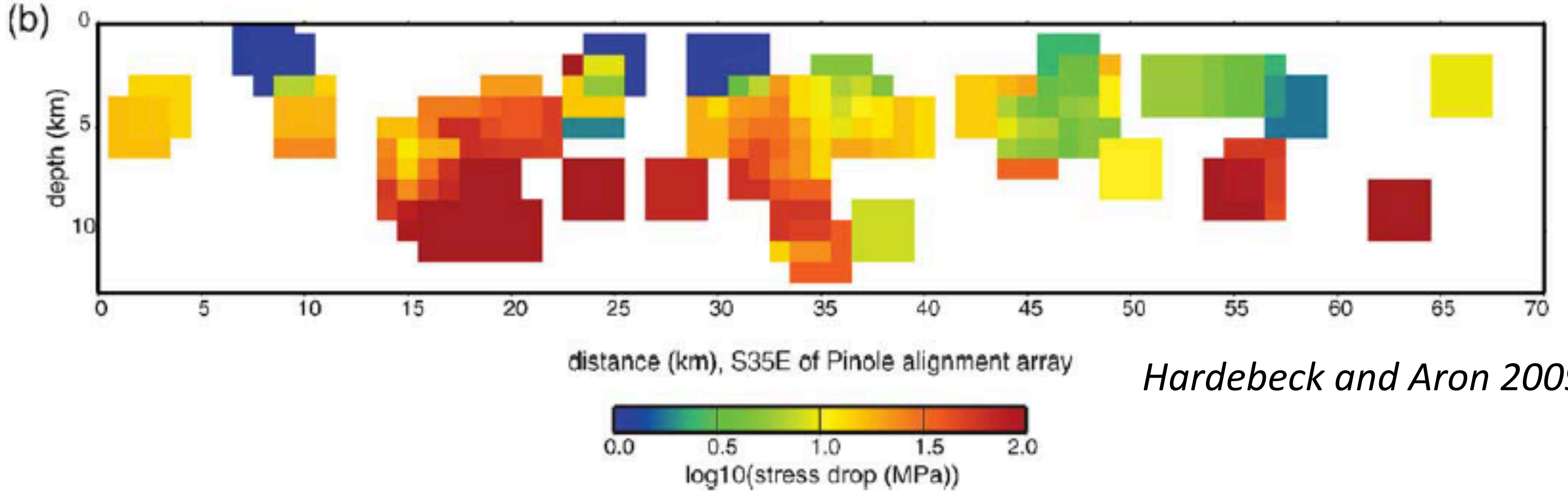

Hardebeck and Aron 2009

Figure 10. (a) Stress drops of individual earthquakes within 5 km of the Hayward fault, shown projected onto the fault. Distance measured along the fault southeast of Pinole (37.9891°, −122.3546°), shown in Figure 1, assuming the fault strike is N35°W. (b) Average stress drop in 1 × 1 km bins on the Hayward fault surface, smoothed using a moving window of 3 × 3 km. Averaging done in the log domain.

Thank you for your attention

ACKNOWLEDGEMENTS
@ ENS: François Passelègue, Raul Madariaga
@ IPGP: Harsha Bhat
@ INGV Roma: Stefan Nielsen

CONCLUSIONS

Rupture nucleation:

- AEs correspond to microcracking (damage accumulation) - NOT TO RUPTURE

- AE rate prior and post rupture (ie number of Aes and AE rate) follows Omori's law but depend on the lithology and the porosity

- On intact samples, terminal rupture speeds <10m/s, so NOT FULLY DYNAMIC

- Nevertheless, we observe a variety of signals (LFAEs)

CONCLUSIONS

Dynamic rupture propagation :

- SS and SR can be spontaneously reproduced on saw cut samples, both in resin and Rocks. SR happens at low prestress, SS at high pre-stress

- Rupture velocity can be determined using either images or acoustics independently

- Radiation due to dynamic rupture propagation is at least four or five orders of magnitudes larger than that produced by nucleation (or precursors)

- Introducing a kink, one introduces complexity (and HF)

- The experiment scales reasonably well with nature, except for slip.

- Even for a few tenths of mm slip, frictional heating term becomes predominant so that rupture becomes more dissipative and one can observe changes in the mineralogy

II. Dynamic propagation in ROCKS!!

Comparison with dynamic rupture propagation – Far-field sensors
(simulation code by Eric Dunham, courtesy Harsha Bhat, Steady state self healing pulse)

Vr = 0.8Cs

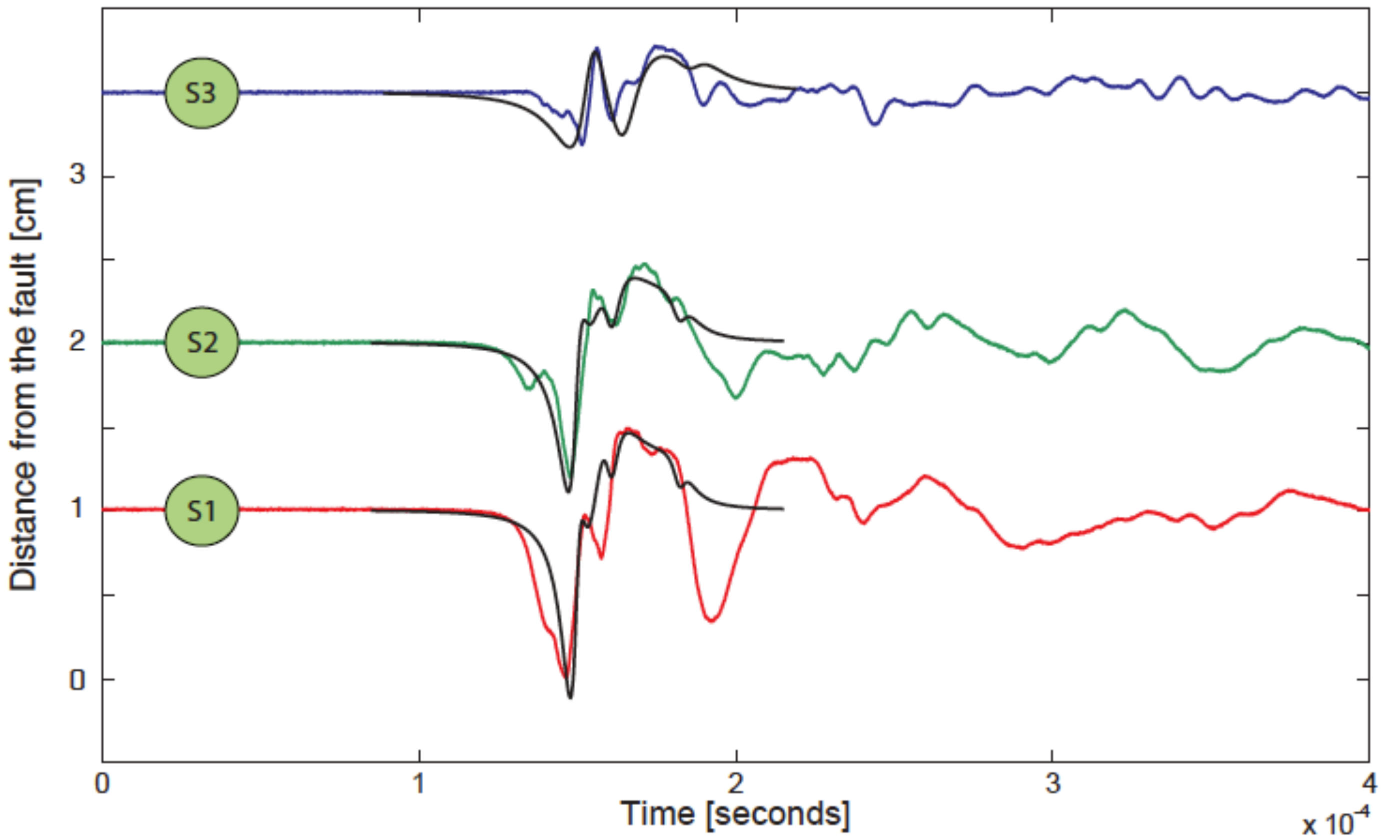

II. Dynamic propagation

And the waveforms compares with real recordings!

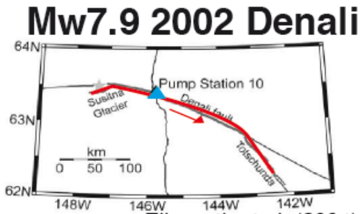

Ellsworth et al. (2004)

Analog to the experiments:
- Super-Shear speed
- Accelerometric data at PS10
- Two kinks

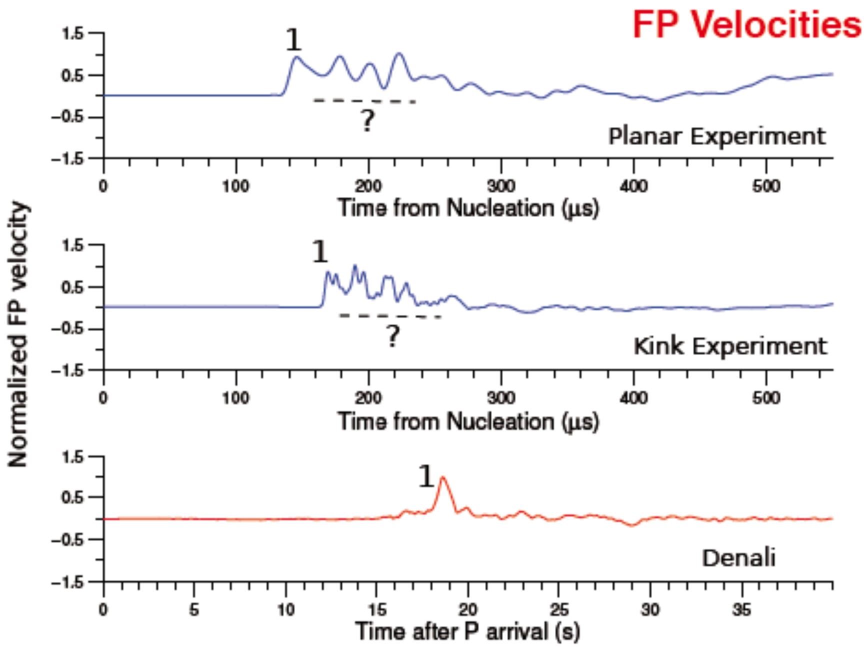

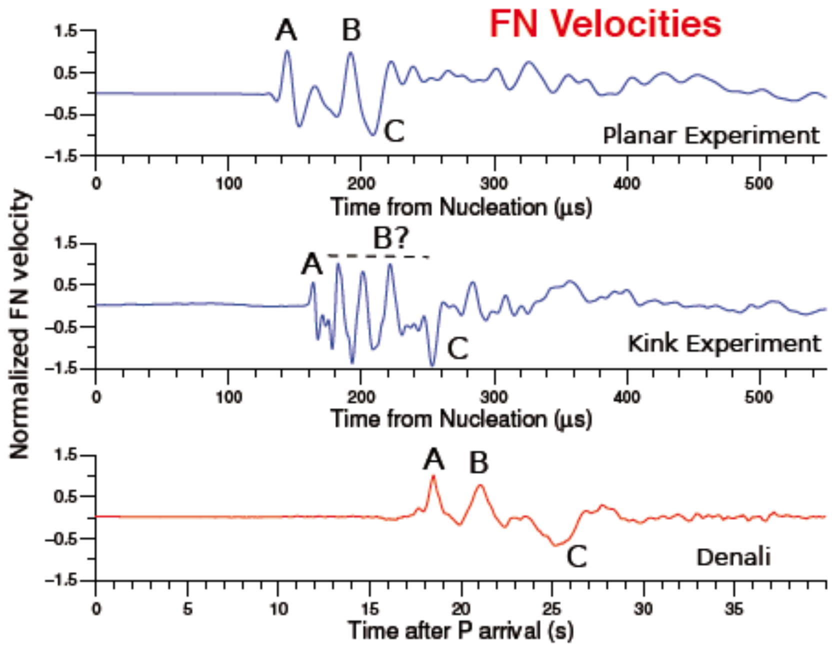

Chanard et al., 2011

A - pulse like super-shear rupture (energetic Mach front)
B - Most probably Rayleigh waves
C - Trailing Rayleigh rupture propagation?

II. Dynamic propagation

Experiment scales with nature

Mw7.9 2002 Denali

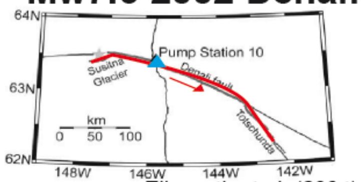

Ellsworth et al. (2004)

Analog to the experiments:

- Super-Shear speed
- Accelerometric data at PS10
- Two kinks

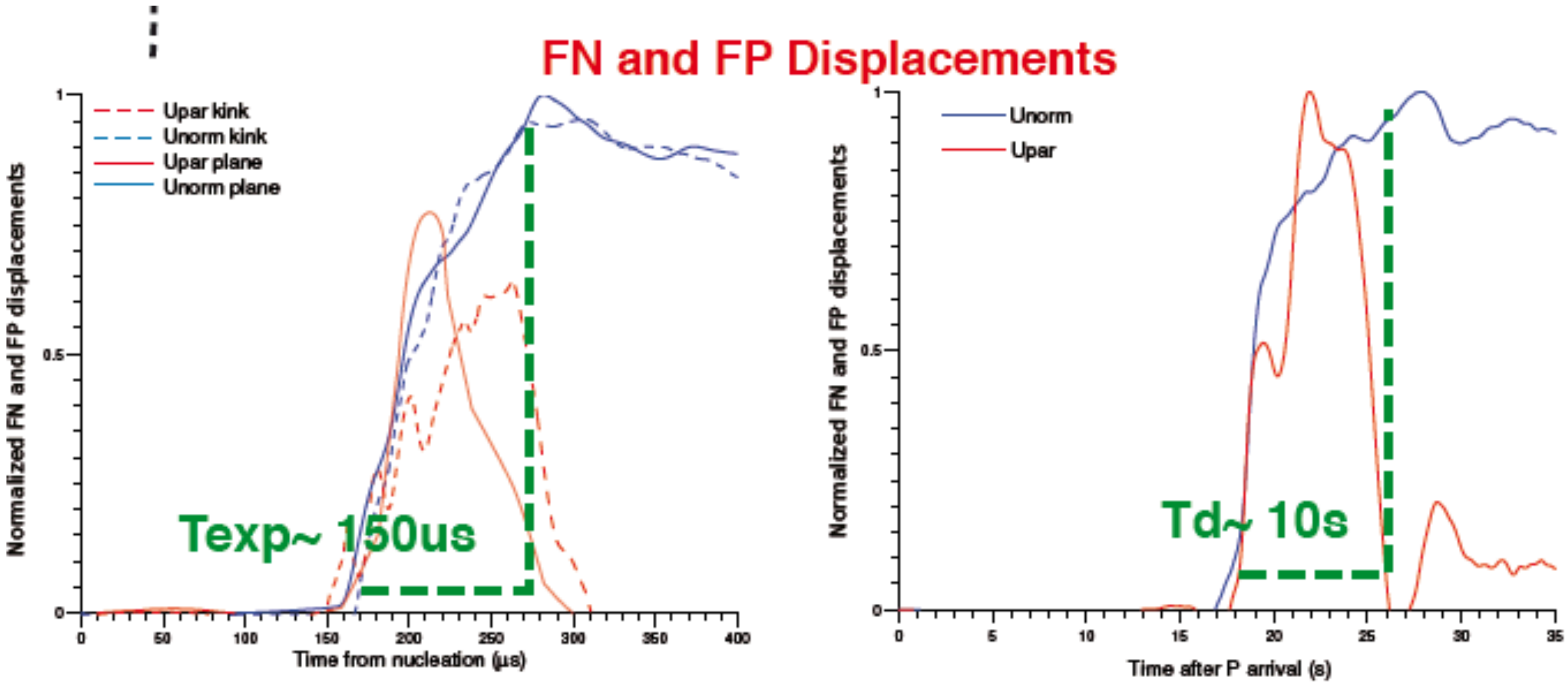

$$\frac{\tau_{exp}}{\tau_D} = \frac{V_D \times L_{exp}}{L_D \times V_{exp}} \sim \frac{5km/s \times 30cm}{100km \times 1km/s} \sim 1.5 \times 10^{-5}$$

Chanard et al., 2011

$150\mu s$ in experiment $= 1s$ in nature

BUT 100 microns of slip only!

III. High Velocity Frictional sliding

HVF apparatus in Hiroshima University

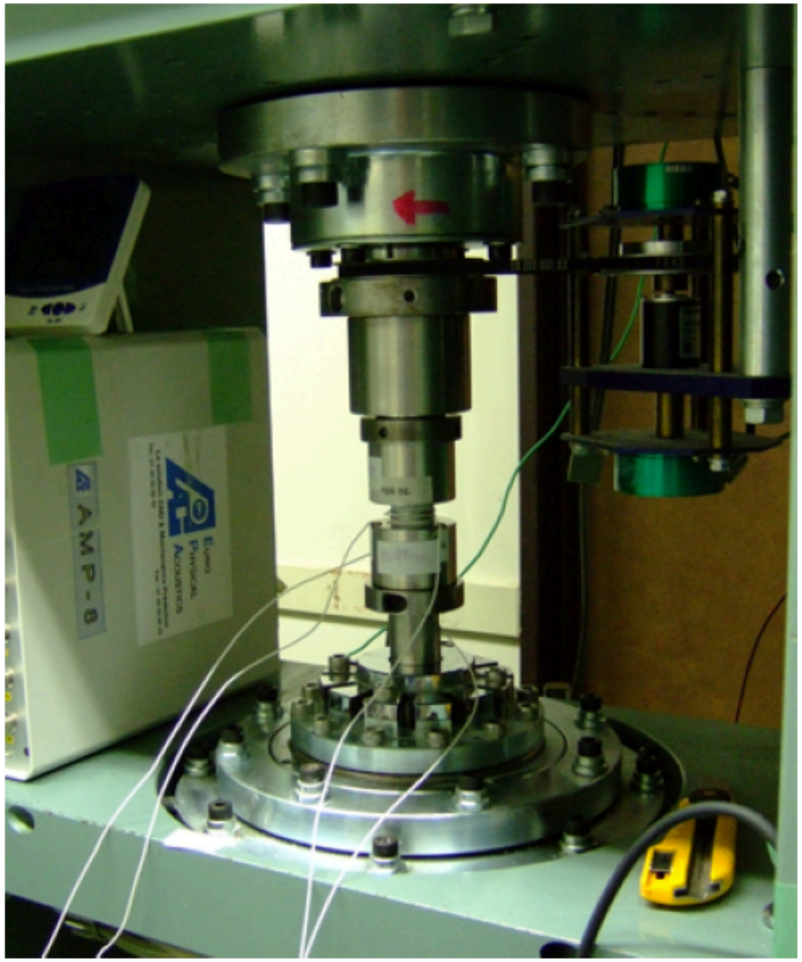

III. High Velocity Frictional sliding

Sample preparation

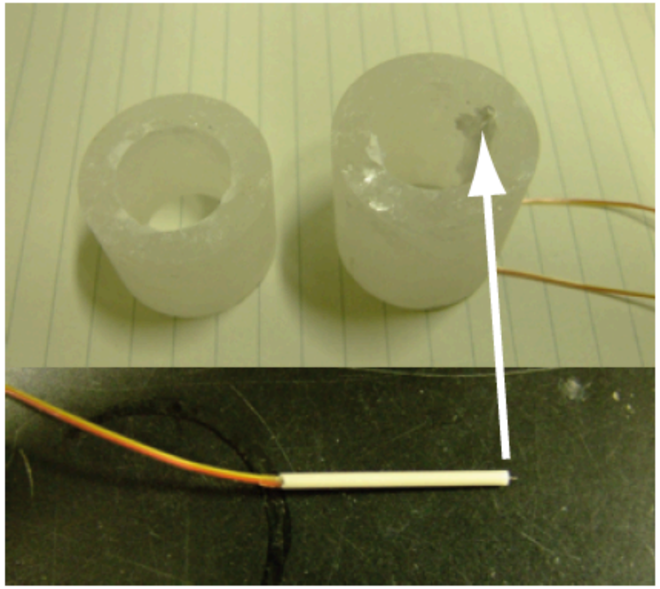

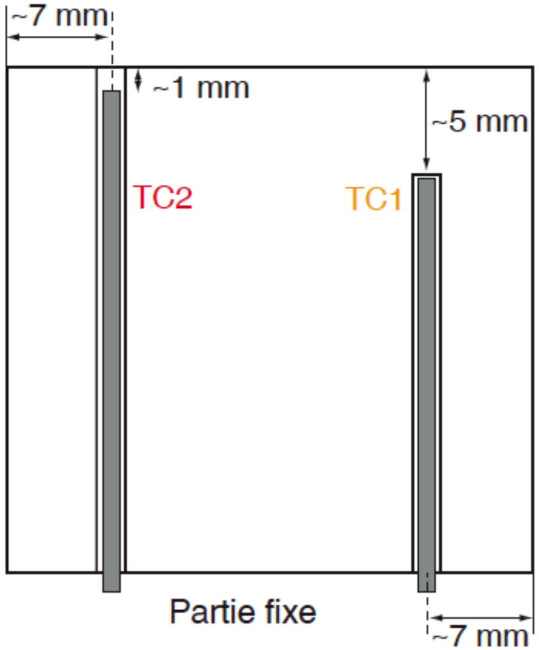

We choose gypsum since it dehydrates at a temperature close to ambient T. Each sample is prepared with one or two thermocouples, located

- as close as possible from the sliding surface
- at a distance of around 5 mm from the SS

III. High Velocity Frictional sliding

III. High Velocity Frictional sliding

Thermal behaviour

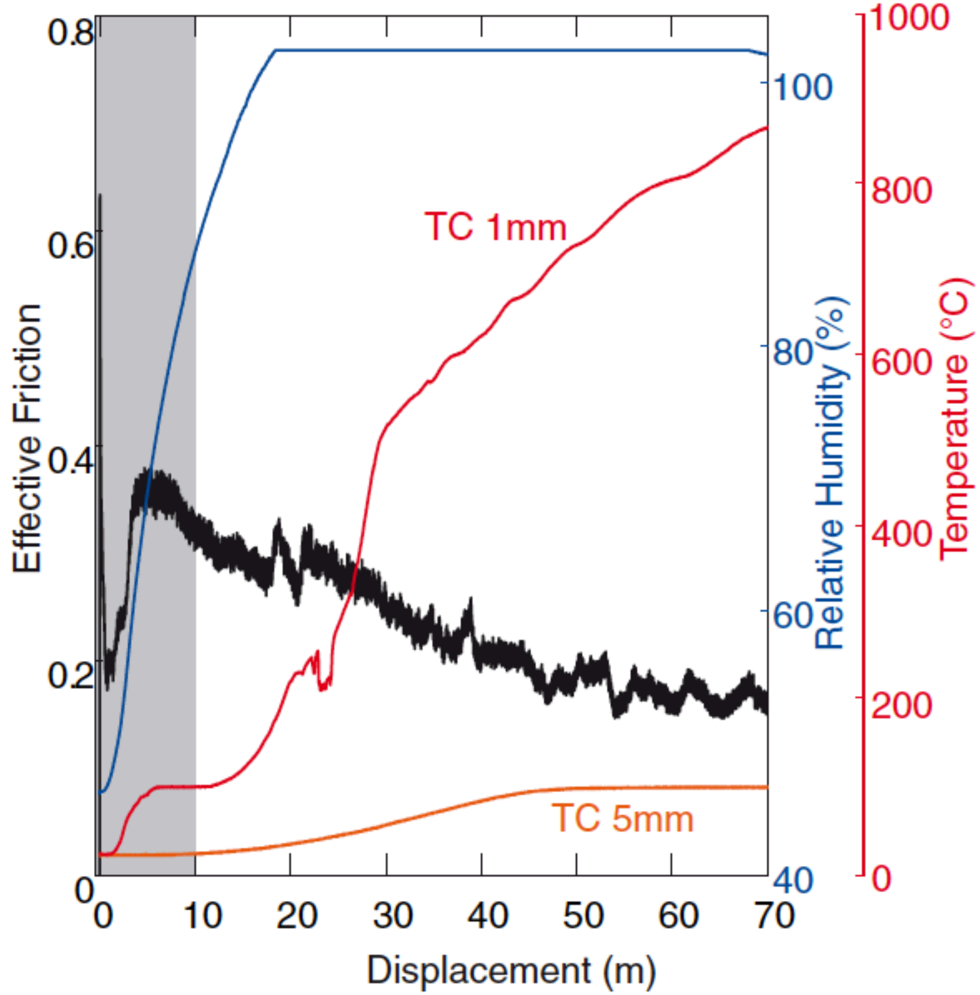

Experimental Conditions

Solid cylinder, Normal Stress 2 MPa, Speed 1.3 m/s, Unconfined atmosphere, Temperature mesured with 2 thermocouples.

Brantut et al., 2011

III. High Velocity Frictional sliding

Microstructures

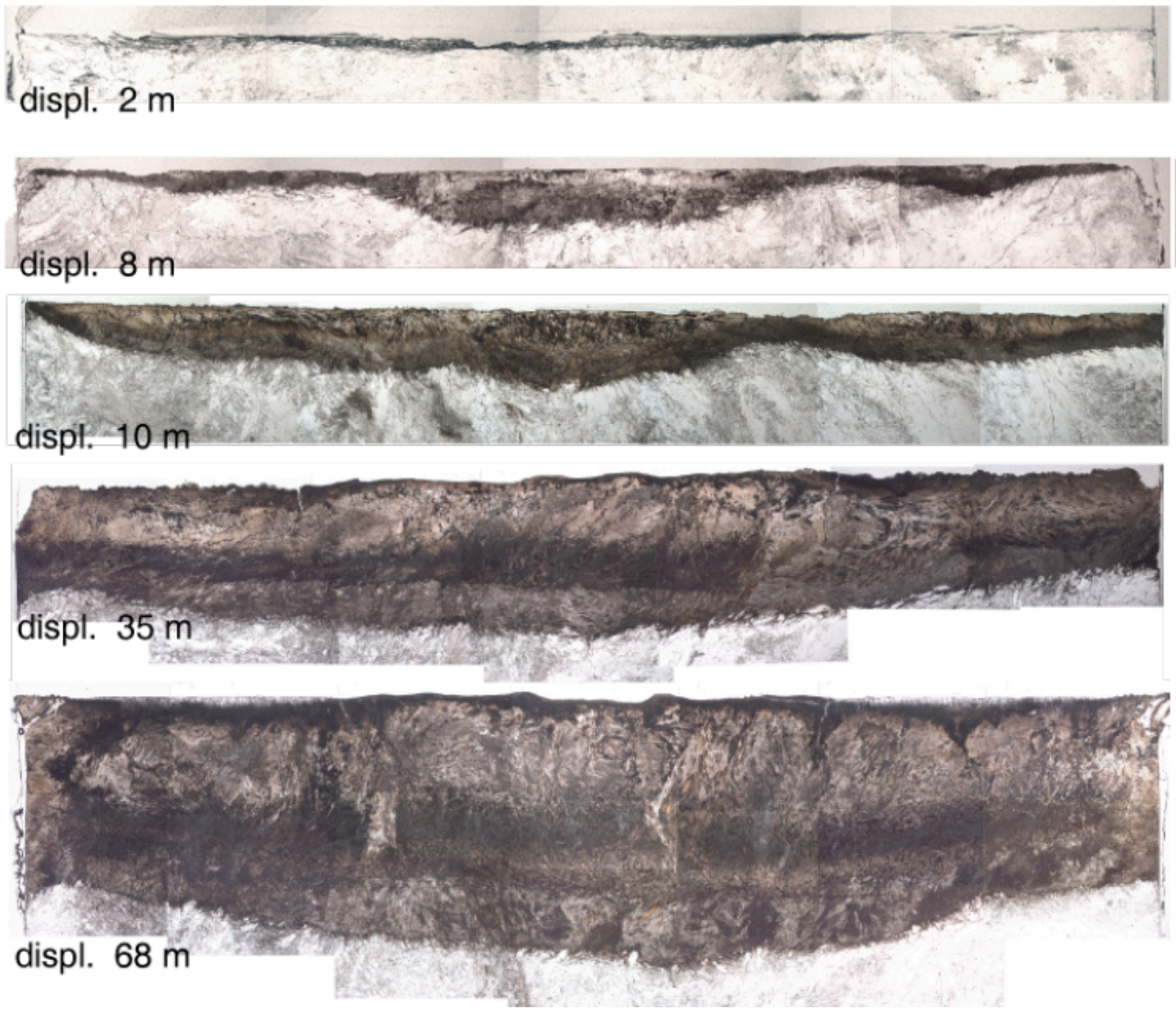

Brantut et al., 2011

Off fault damage

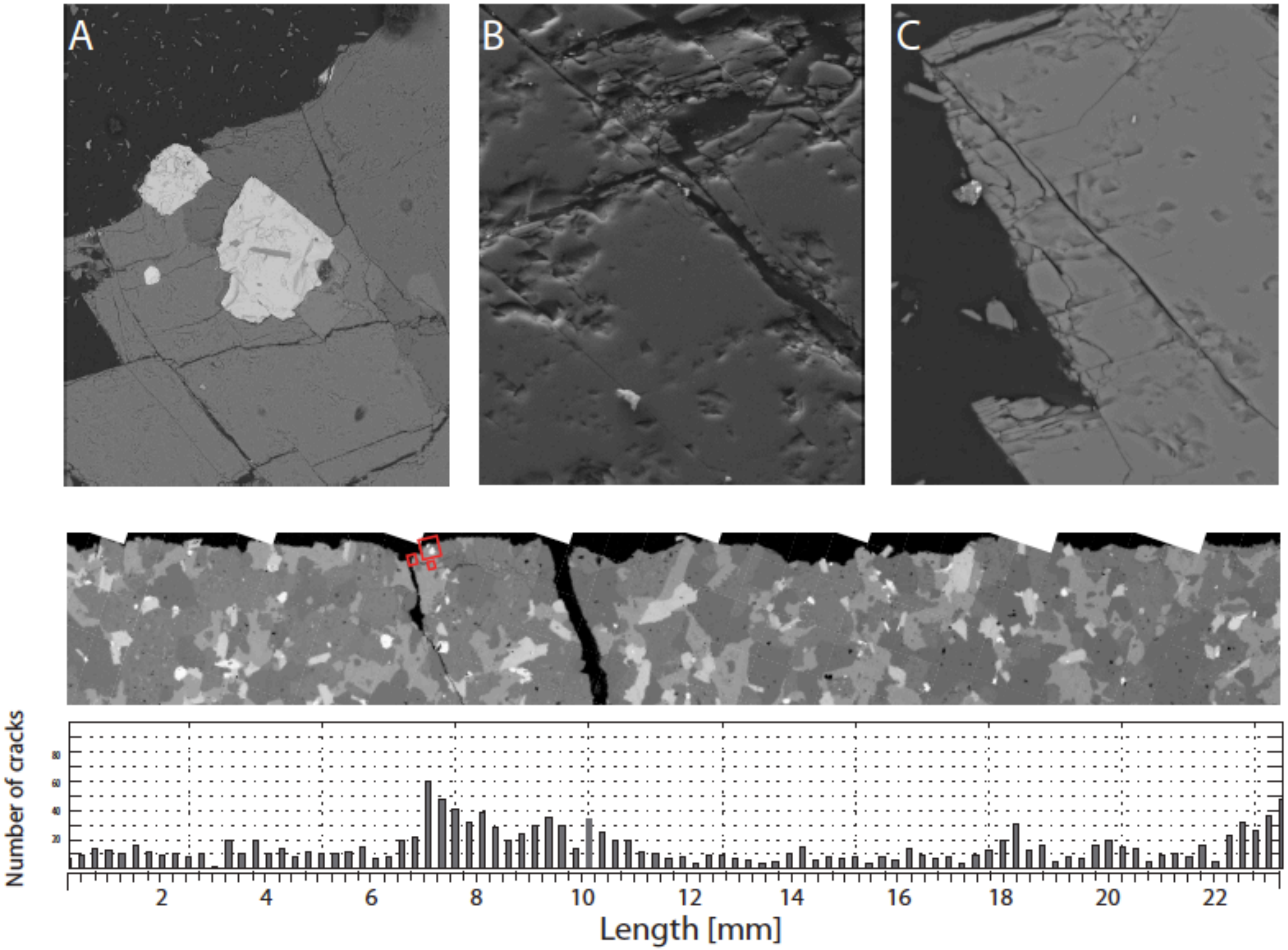

III. High Velocity Frictional sliding

X ray diffraction

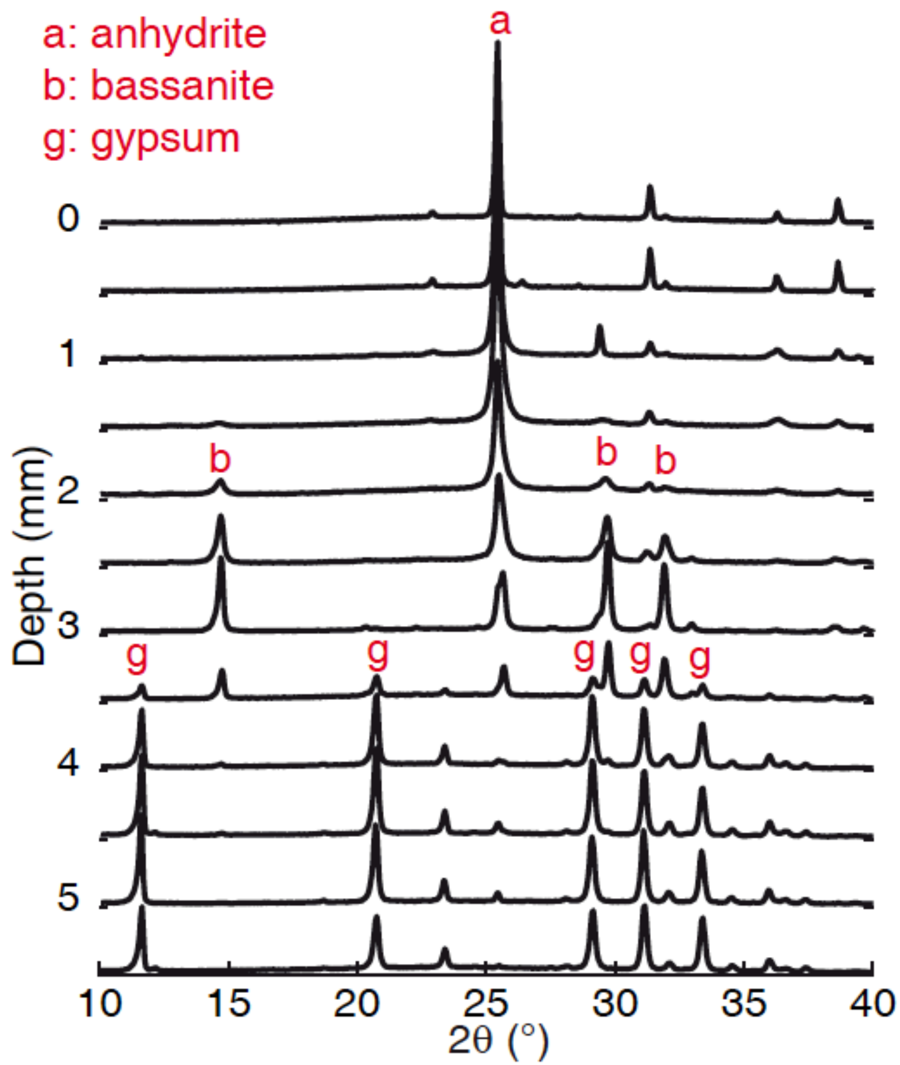

Brantut et al., 2011

III. High Velocity Frictional sliding

Amount of energy taken by dehydration

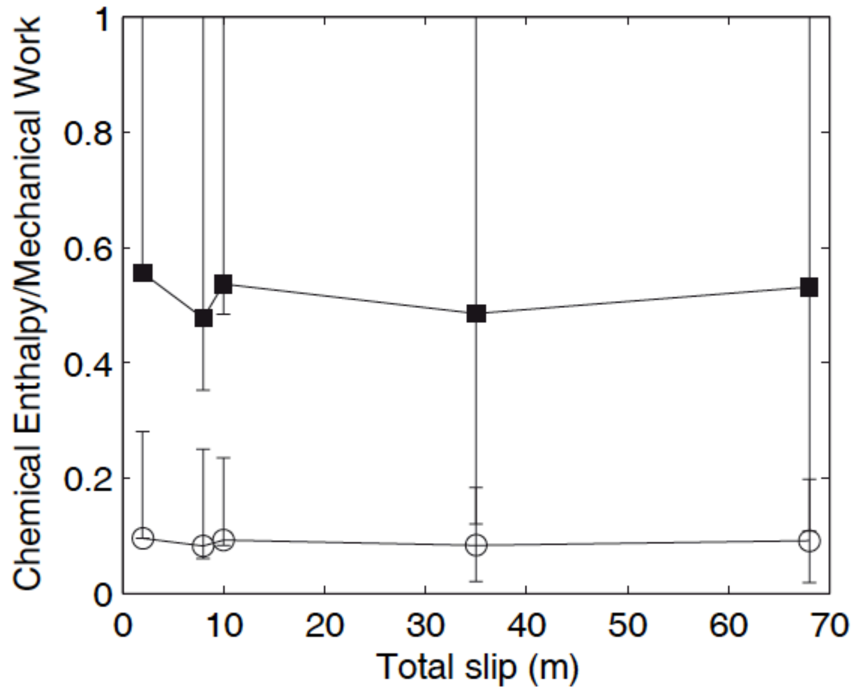

Brantut et al., 2011

Between 10 to 50% of the total mechanical work is taken by the reaction.
Other energy sinks/loss: diffusion, temperature increase...

II. Dynamic propagation

Introducing a 2° kink introduces complexity

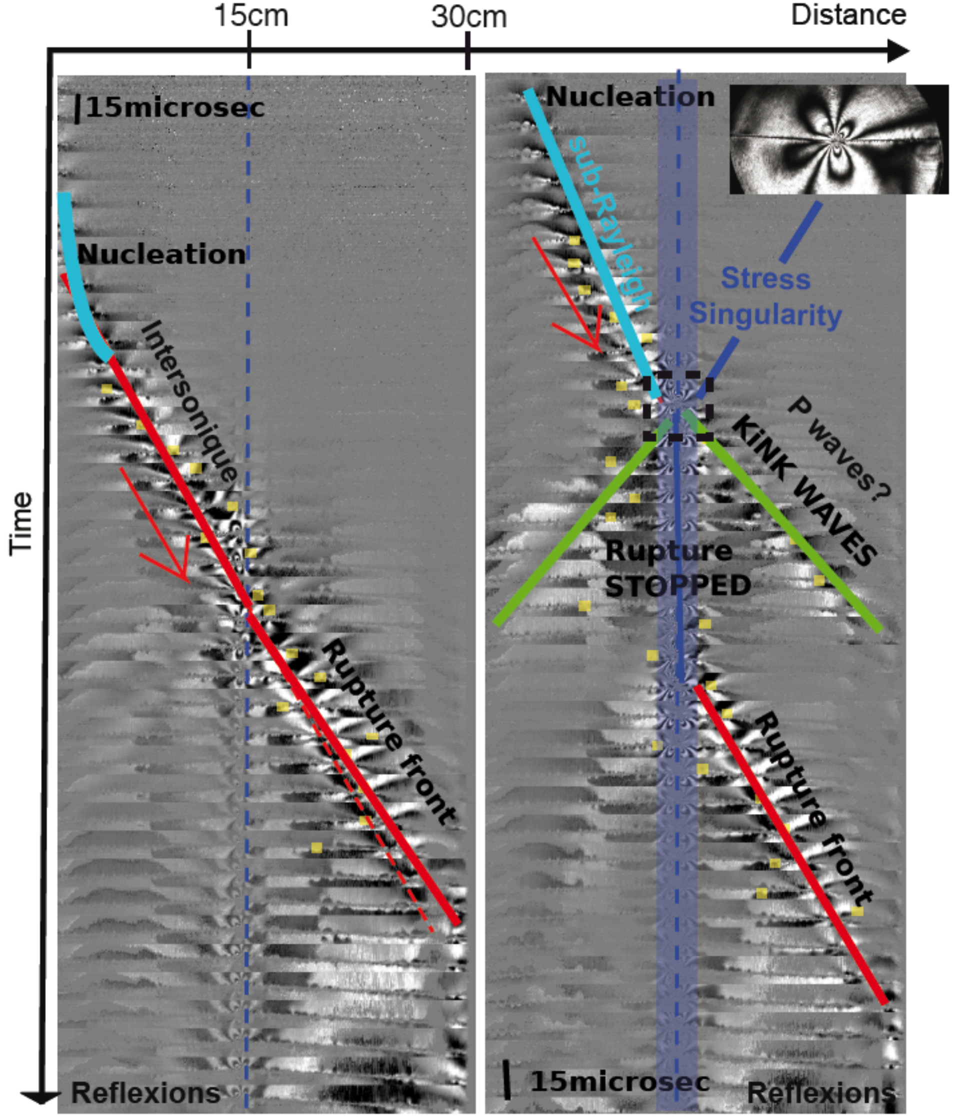

Figure 8: Series of interferometric photograms recorded by the high velocity camera for events stopping or not at the singularity

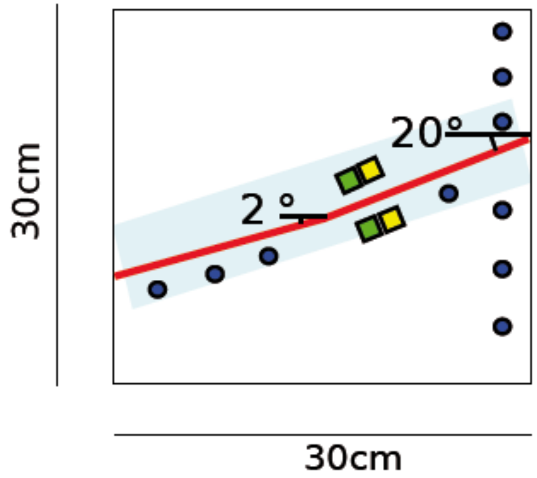

Chanard et al., 2011

II. Dynamic propagation

Introducing a 2° kink introduces complexity … seen in the waveforms

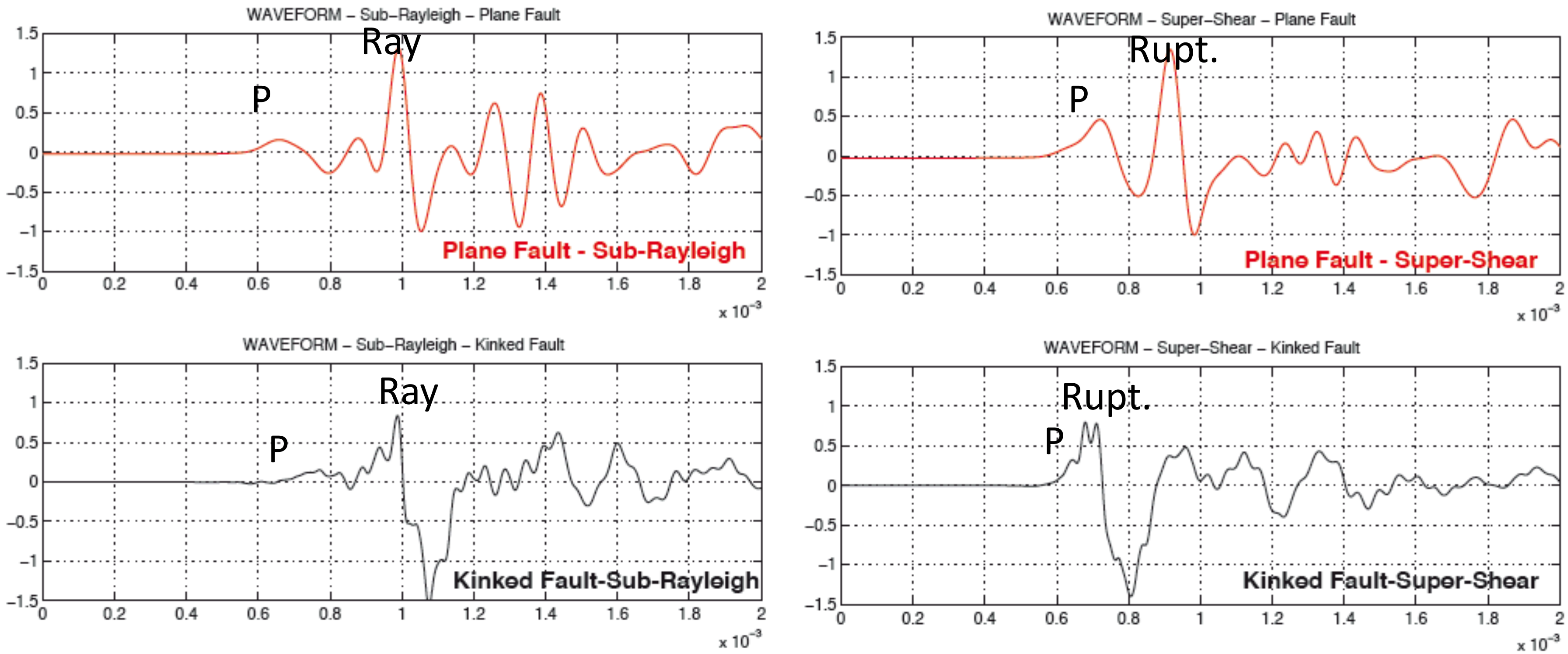

High frequencies generated by the singularity for sub - and super-shear ruptures

Chanard et al., 2011

II. Dynamic propagation

Nucleation and Locations

Quasi static locate on the plane at 22.5 mm
Dynamic locate on the plane at E 104.4

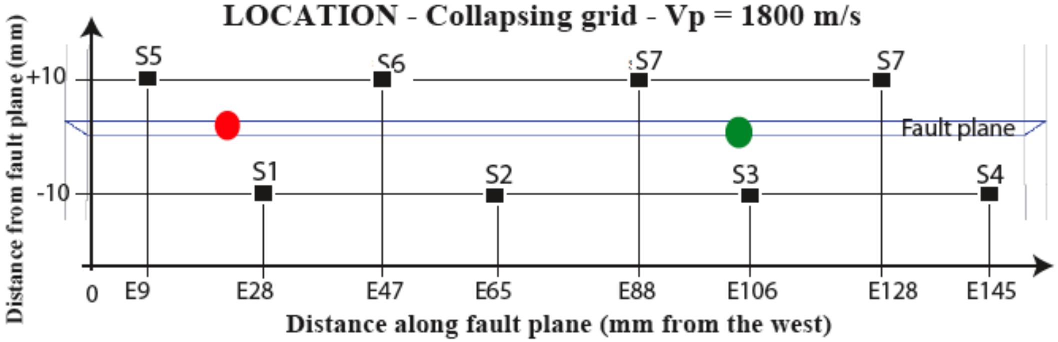

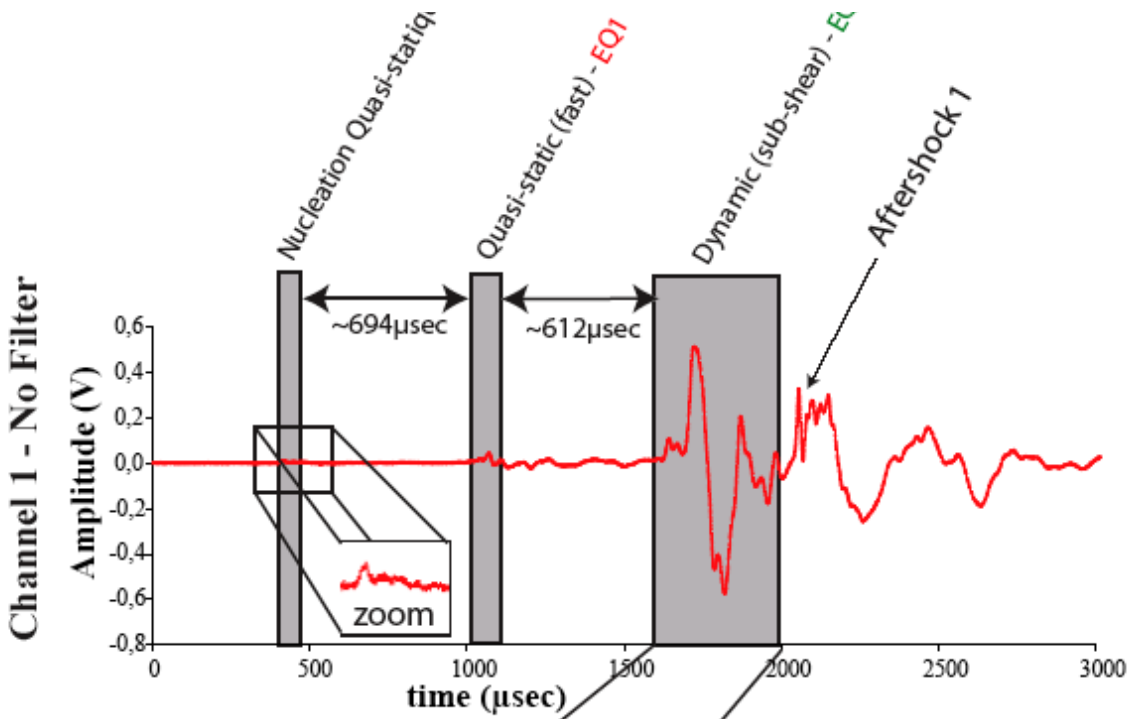

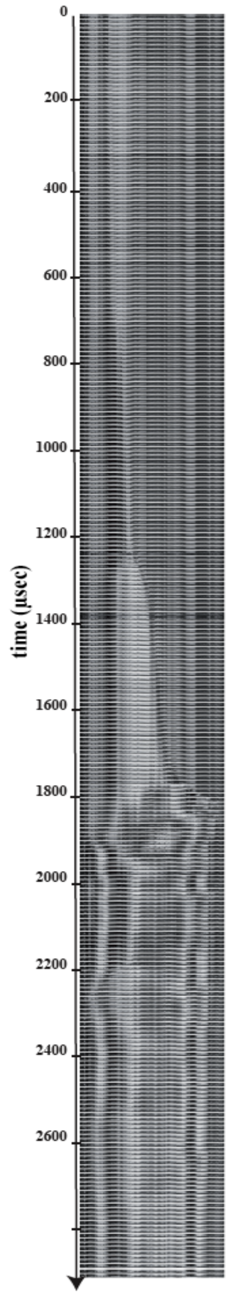

CFMR, Arts et Métiers, Février 2013

II. Dynamic propagation

Hodochrones away from fault - Amplitude of supershear wavefronts
Comparison between experiment and numerical simulation

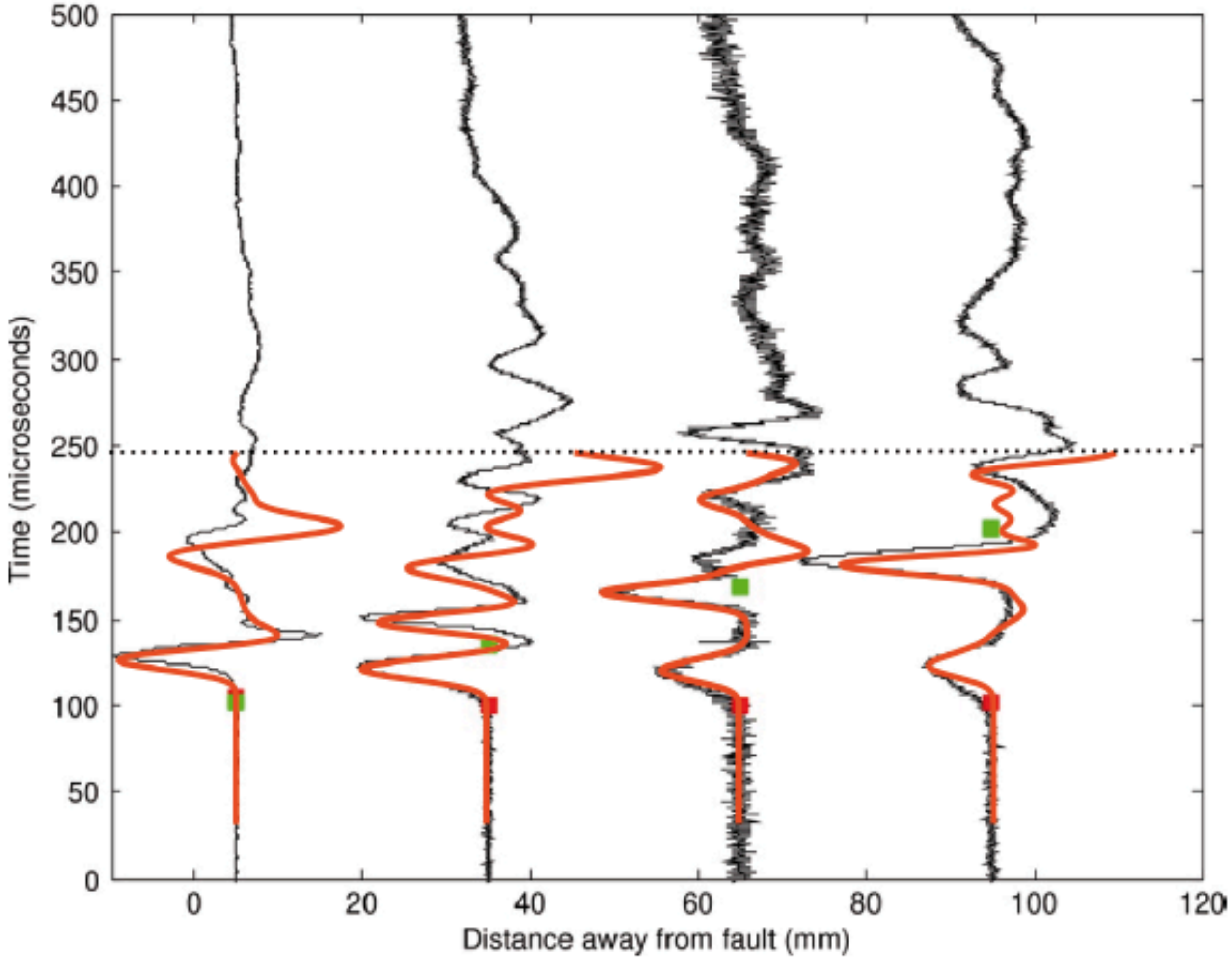

Schubnel et al., 2011